NOVEL SILICONE-BASED MATERIALS TO LIMIT BACTERIAL ADHESION AND SUBSEQUENT PROLIFERATION

NOVEL SILICONE-BASED MATERIALS TO LIMIT BACTERIAL ADHESION AND SUBSEQUENT PROLIFERATION

BY

MADIHA KHAN, H.B.Sc

A Thesis

Submitted to the School of Graduate Studies

in Partial Fulfillment of the Requirements

for the Degree

Master of Applied Science

McMaster University

MASTER OF APPLIED SCIENCE McMaster University

(Biomedical Engineering) Hamilton, ON

TITLE: Novel Silicone-based Materials to Limit Bacterial Adhesion and Subsequent Proliferation

AUTHOR: Madiha F. Khan, HBSc (University of Toronto)

SUPERVISORS: Dr. Michael A. Brook

Dr. Heather D. Sheardown

NUMBER OF PAGES: xi, 86

.

ABSTRACT

Bacterial biofilms are problematic in a variety of industries hence strategies for their mitigation have received significant attention. The approach described herein attempts to control bacterial adhesion using silicone-based polymers- (widely used due to their interesting properties)- via manipulation of their surface chemistry to eventually create anti-fouling surfaces. This involved study of the systematic variation of surface wettability and its effect on *Escherichia coli* (*E. coli*) adhesion to novel polymers of acrylate-modified silicone surfactant (ACR) with either hydroxyethyl methacrylate (a hydrophilic monomer), or methyl and butyl methacrylate (hydrophobic monomers). It was hypothesized that the systematic variation of ACR would produce surfaces with differing wettability, without changing other surface properties that influence cellular adhesion. Average light transmittance across the range of visible light wavelengths (400-740nm), surface roughness and Shore 00 hardness data were consistent across the ACR-HEMA copolymer series (80-90%, ~2.5 – 5 nm, and 75-95 Shore durometer points, respectively). The same consistency was observed for surface wettability (contact angles = 78-92°) despite varying HEMA content and consequently *Escherichia coli* (*E.coli*) adhesion, likely due to system saturation with silicon (as confirmed by EDX). However, wettability of the ACR-MMA-BMA polymers did vary; ≤ 20 wt% and ≥ 80 wt% ACR polymers had contact angles between 67°- 77°, while $20 < x < 80$ wt% ACR polymers had increased surface wettability (contact angles 27.6°- 42.9°). *E. coli* adhesion across the set increased with increasing ACR content, a trend mirrored by the water uptake of the

materials but not the contact angle data. These results indicate that *E. coli* adhesion occurs independently of wettability for these materials and although the effect of the latter on adhesion cannot be deduced, the possible correlation between bacterial adhesion and water uptake suggests that the best antifouling surfaces should not be of materials capable of imbibing significant amounts of water.

ACKNOWLEDGEMENTS

I have long believed that we are a product of our cumulative experiences, whether situational or interpersonal. So when celebrating milestones in life it is often difficult to appropriate thanks- where does one begin and where does one find the words to express their overwhelming gratitude? Though this section provides insufficient space to properly credit all those responsible for my very modest achievements to date, try I must with the hope I will be forgiven by those I could not acknowledge.

First and foremost, I must thank my co-supervisors Michael A. Brook and Heather D. Sheardown, who are lauded not just by their students, but also by the many faculty and staff with whom they interact. I remember being stunned into silence early in my Masters when Dr. Sheardown kindly said, "you will need to teach Mike and I about bacteria". *Me*? Teach two people with individual lists of achievements longer than I am tall about *anything*? Impossible! And I remember glancing at Dr. Brook waiting for the laughter that would conclude this joke-of-the-year. But the laughter never came. That for me characterizes the environment fostered by my supervisors for their students- one of open dialogue and good-humored collegiality, with a sense that challenges big or small are more fun and better-solved when tackled together.

In particular I need to thank Dr. Brook for his extraordinary patience and support. I shall forever feel indebted to him for housing a biologist in his chemistry lab and for granting me the incredible learning opportunities that he has. No amount of work on my part could repay his kindness.

Of course the learning might have been impossible if not for the amazing individuals in the Brook lab. Special thanks goes to Laura Dodge for her practical and timely guidance (truly a brilliant instructor in the making), Anna Szelag for her inspiring faith, Alex McLaughlin for his stories and books, Martin Sweetman for his gracious wisdom and brainstorming sessions, Ferdinand Gonzaga for his company during weekends in the lab, Vinodh Rajendra for his help with EDX (and for perpetually stealing time from my meetings with Mike), Marlena Whinton for teaching a biologist how to synthesize materials, and Alan Vanderkooy for the privilege of his friendship.

Then there are the professors and staff from my time at the University of Toronto who encouraged a socially awkward young girl to dream, (Jane Ngobia, Rory Hinton, Angela Lange, Nicholas Collins, Harvey Shear, Brian Branfireun, Jacqueline Brunning and Sue Prior), the incredible friends who inspired her to chase those dreams (Varun Gupta, Adam Edris, Elrika, Oey, Fatima Ul-Haq, Dania Aldouri, Anthony Scolaro and Marco Maseellal) and most importantly, her family and parents, whose unconditional love and prayers shone through her shadows of self-doubt to illuminate the path of pursuit (without you Mum and Dad, I am nothing).

To all these people and those unmentioned but loved as dearly, I owe an incredible debt of gratitude. One day I will justify your trust and make you proud.

TABLE OF CONTENTS

LIST OF FIGURES

LIST OF TABLES

1. Chapter 1: Introduction

1.1. Bacterial Biofilms

Bacteria (and most other microorganisms) exist in one of two states: **planktonic** (free-floating or swimming in aqueous solution) and **sessile** (stationary microcolonies on a living/non-living solid substrate).[1] The latter state is an evolved defense mechanism against hostile environments in which bacteria (0.2-2µm x 1-10µm)[2] are susceptible to antagonists.[3] Typically the sessile or 'stationary microcolonies' state of existence for bacteria predominates.[2]

The irreversible adhesion of multiple microcolonies to the same substrate surface is termed a **biofilm**. These films can be comprised of a single species of bacteria or multiple, metabolically cooperative species.[2] Both types are protected by a homogenous, fibrous exopolysaccharide matrix,[4] which allows a 1,000-fold increase in resistance to eradication efforts via biocides, surfactants, predators and antibiotics in comparison to planktonic bacteria.[2,5] This is problematic, since biofilms are ubiquitous and detrimental in various industries where their growth is undesirable. For example biofilm formation, also known as biofouling, impedes physical operational efficiency by blocking filters and reducing the flow capacity of pipes.[6] It can spoil petroleum products by changing the bulk fluid composition or increasing the amount of suspended solids.[6] In addition, biofilm formation on food or surfaces in contact with food can cause health issues and economic losses due to food spoilage.[7,8]

1.2. The Medical and Global Health Context

Microbial biofilms are equally problematic in the biomedical industry. Their formation on medical implants prevents normal removal of opportunistic bacteria by phagocytosis, since bacterial antigens inside the matrix are suppressed.[9] Additionally, biofilm pathogens dispersed from the matrix after complete maturation [Figure 1] may elicit disease processes elsewhere in the body.[10] The matrix itself can provide a niche for antibiotic-resistant species[11] while device-associated infections significantly increase the risk of mortality, as is the case when infected stents physically block blood vessels. [12]

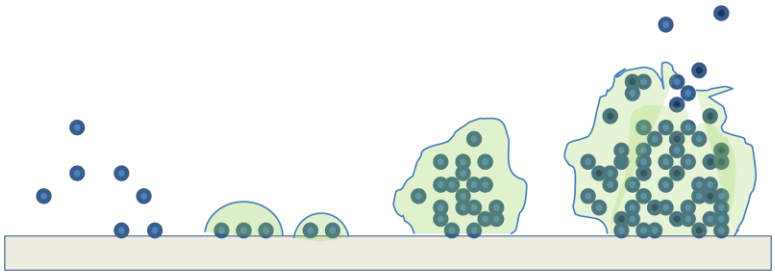

Figure 1: Biofilm formation and maturation. Planktonic bacteria settle on a suitable surface, form microcolonies encased in a protective exopolysaccharide matrix, and subsequently escape from the mature biofilm to settle elsewhere.[10]

Biofilms can also undermine the integrity of medical devices through mechanical and chemical degradation, which results in device failure and a need for replacement.[13] Costs associated with infection of medical implants such as orthopedic devices and mechanical heart valves range from $15,000 to more than $50,000 per occurrence, respectively.[14] In the broader context, the ability of biofilms to colonize household surfaces (such as water collection vessels) coupled with poor disinfection and hygiene

practices in developing countries further exacerbates the prevalence of water-borne diseases such as cholera in those regions.[15]

Consequently, given the burden biofilms place on health care, along with their potentially fatal consequences, much work has been done on developing biofilm resistant surfaces. Current strategies include altering the physiochemical properties (such as hydrophobicity, surface charge and surface roughness)[16] of the material to limit initial bacterial adhesion, and more commonly, incorporating known antibiotics into the implant.[17] The principal problem with the latter strategy is achieving controlled release kinetics; most of the agent is discharged early after implantation with the remainder being released more slowly over time.[15] In the worst case, this exposes bacteria to sublethal doses of antimicrobials that can facilitate the production of resistant strains.[15] There is evidence that devices coated with hydrogels or antimicrobial peptides have all proved to be largely ineffective,[18] while the use of silver salts as an antibiotic in controlled-release devices and polymer coatings, which has received significant attention recently, remains a concern due to the possibility of adverse affects on surrounding human tissue.[19,20] As a result, this thesis focuses on the first strategy, involving alteration of a material property.

1.3. Silicon Materials in the Biomedical Industry

For the material need described above silicon-based substrates, including silicones, may be the best candidates. Silicones are synthetic polymers comprised of a chain of repeating units of silicon to oxygen bonds (termed ‘siloxanes’) with organic (typically methyl groups) bonded to the silicon atoms[17,21] **[**Figure **2].** The combination of an

inorganic, flexible backbone and organic groups confers interesting properties to these materials allowing their use in a variety of forms such as fluids, resins, emulsions and compounds.[17] Silicones are easily solidified to three-dimensional networks via cross-linking between chains with radical, moisture cure or platinum-catalyzed curing.[22] Characteristics commonly attributed to them and their derivatives are high chemical, oxidative and thermal stability,[23,24,25] hydrophobicity, permeability to gases, durability, transparency and low toxicity (biocompatibility),[26,27] and moldability as a result of their low glass transition temperature and flexibility before cross-linking.[28]

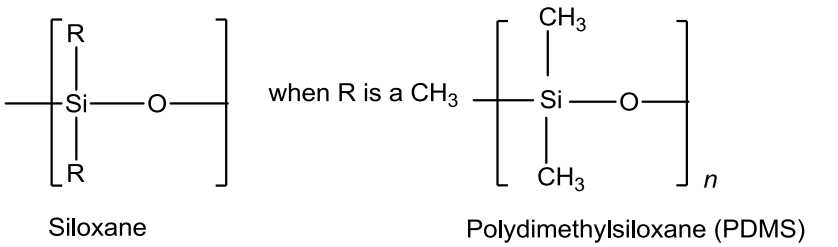

Figure 2: **Repeating unit of polydimethysiloxane (Adapted from Ratner et al.[17])**

For all of these reasons, silicone materials have gained popularity in the biomedical industry and have evolved in pace with emerging needs. Their applications range from lubricants for syringes and implantable hydrocephalus shunts[17] to drug-carrier systems in the form of silica nanoparticles[29] (silica being the oxide of silicon and the most common mineral on Earth). Consequently, some progress has already been made towards creating biofilm-resistant surfaces using silicon-based materials,[30,31,32] and bioencapsulation with the same of proteins,[33] drugs[34] and more importantly living cells[35]

has been demonstrated. In the following thesis, I describe an attempt to control bacterial adhesion by manipulating the surface chemistry of a novel silicone material.

2. Chapter 2: A Systematic Study of Bacterial Adhesion as a Function of Surface Wettability

2.1. Introduction

Although several competing factors influence bacterial adhesion to biomaterials,[36] the hydrophobicity of surfaces in facilitating this phenomenon has received particular attention.[37,38,39] Silicones are notably hydrophobic, since the flexibility of their siloxane backbones enables them to reorient at material-air interfaces to expose their methyl groups.[40] Consequently, the hydrophobicity of silicone materials can be problematic for specific applications, such as the insertion of urinary catheters or intraocular lenses[41], where severe infections of the eye caused by bacterial adhesion may necessitate surgical intervention. However, the *extent* to which hydrophobicity governs bacterial adhesion over other factors is largely unclear, since most existing studies compare bacterial adhesion on different hydrophobic and hydrophilic biomaterials, for example, poly(methyl methacrylate)(PMMA) versus silicone (polydimethylsiloxane)(PDMS) versus hydrophilic acrylic such as poly(hydroxyethyl acrylate)(pHEMA),[42] and the differences between their material properties are likely confounding variables. As of yet, it appears that no published study systematically analyses the effect of surface wettability (hydrophobicity/hydrophilicity) on bacterial adhesion by varying the constituent monomers of a single polymer, and this provides the rationale for this first project.

A small acrylate-modified trisiloxane surfactant (Silmer ACR A008-UP, henceforth referred to as ACR) [Figure 3] was selected for copolymerization with a

known hydrophilic monomer hydroxyethyl methacrylate (HEMA)[43]. Given that relatively small trisiloxane surfactants are known to have high rotational-diffusion coefficients and linear transport through materials to the air-polymer interface,[44] it was hypothesized that ACR would preferentially exist at the surface, but that the amount present could be decreased via the systematic addition of HEMA, since this would cause an overall decrease in the system's ACR content [Figure 3]. In so doing it was thought that a series of copolymers with controlled surface wettability could be produced that would then be amenable to a study of bacterial adhesion as a function of surface wettability.

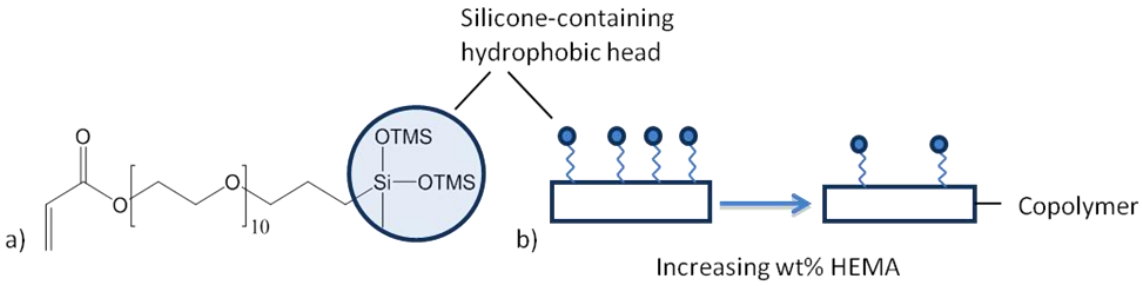

Figure 3: Schematic showing a) the chemical structure of the acrylate-modified silicone surfactant (Silmer ACR A008-UP); and b) the theoretical (proposed) decrease of ACR at the air-surface interface upon the systematic addition of hydroxyethyl methacrylate (HEMA) due to a dilution effect.

2.2. Materials and Methods

2.2.1. Materials

Silmer ACR A008-UP (ACR) was a gift from the Siltech Corporation and stored at -20 °C until needed. Diethylene glycol diacrylate (DEGDA), 2- hydroxyethyl methacrylate (99%) monomer (HEMA), 2,2-dimethoxy-2-phenylacetophenone (99%) radical photoinitiatior (DMPA), and hydroquinone monomethyl ether (MEHQ) inhibitor

remover were purchased from Sigma Aldrich. Inhibitors were removed from the HEMA monomer via passage through a MEHQ-packed column and stored in an amber bottle at 4 °C along with the DEGDA. A Sylgard®184 Silicone Elastomer Kit was obtained from Dow Corning to create polydimethylsiloxane (PDMS) elastomers. A K-12 strain of *Escherichia coli* (*E. coli*), capable of producing Green Fluorescent Protein (GFP) after induction with Isopropyl β-D-1-thiogalactopyranoside (IPTG), was obtained from the Promega Corporation (Madison, WI, USA).

2.2.2. Copolymer Synthesis

All copolymers were synthesized to have a final weight of ~2 g, 0.5 weight percent (wt%) DMPA and 1 wt% DEGDA, while the wt% ratios of HEMA and ACR were varied to create copolymers of 60, 65, 70, 75 and 80 wt% ACR. The general polymer synthesis [Figure 4] is exemplified with the procedure for creating a 60 wt% ACR copolymer.

DMPA (0.5 wt%, 0.1 g) and inhibitor-free HEMA (40 wt%, 0.8 g) were weighed into a glass vial that was capped and mixed for 10 min at 120 rpm, or until complete dissolution of DMPA in the HEMA was apparent by eye. ACR (60 wt%, 1.2 g) and DEGDA (1 wt%, 0.02 g) were subsequently weighed into the vial and the mixture was purged with nitrogen (N_2) gas for 1 min to deoxygenate the system. The vial was capped and the contents were homogenized by a further 10 min of mixing, followed by another 1 min of purging with N_2 (g). The resultant solution was transferred into a Teflon-lined, 35 mm x 10 mm polystyrene Petri-dish and irradiated with UV light at 254 nm for 30 min under a N_2 atmosphere. This procedure was repeated to synthesize solid elastomers with

different ACR weight percentages, a summary of which can be found in Table 1. The synthesis of poly-ACR and poly-HEMA followed the same protocol without the addition of the co-monomer to the mixture.

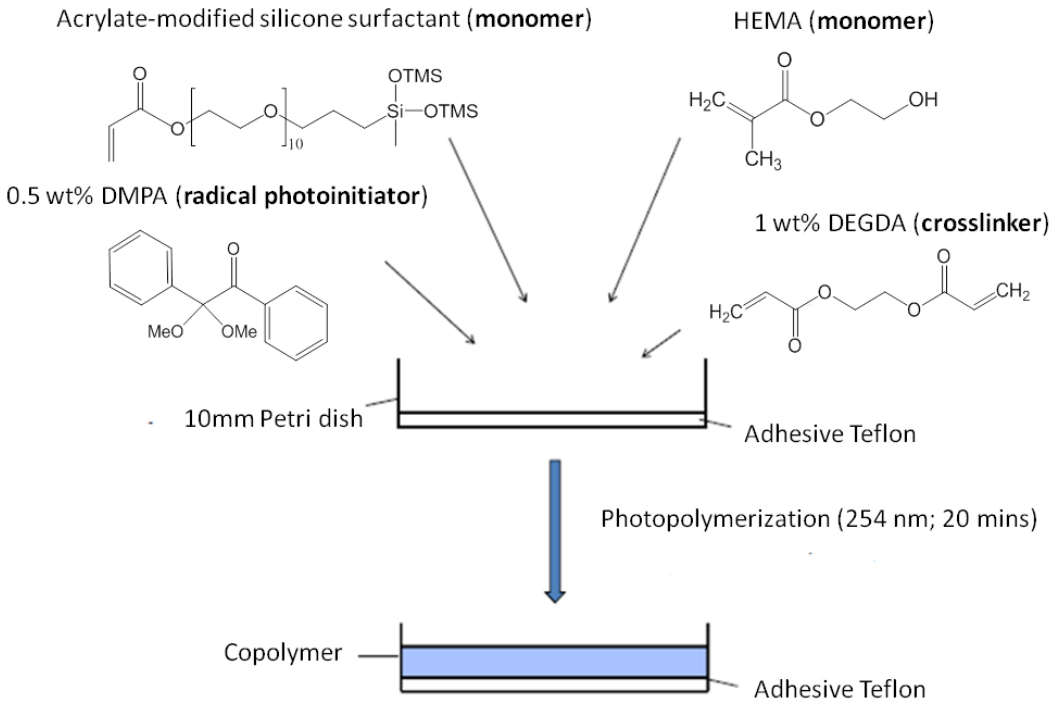

Figure 4: Schematic for copolymer synthesis. The procedure was used to create copolymers of 60, 65, 70, 75, 80 wt% acrylate-modified silicone surfactant (ACR), poly-HEMA and poly-ACR. The latter two served as controls for biological studies.

Table 1: The compositions of the synthesized copolymers and controls.

	Polymer						
Reagent	**Poly-HEMA (g)**	**Poly-ACR (g)**	**60 wt% ACR (g)**	**65 wt% ACR (g)**	**70 wt% ACR (g)**	**75 wt% ACR (g)**	**80 wt% ACR (g)**
DMPA	0.01	0.01	0.01	0.01	0.01	0.01	0.01
DEGDA	0.02	0.02	0.02	0.02	0.02	0.02	0.02
HEMA	1.97		0.78	0.68	0.58	0.48	0.38
ACR		1.97	1.19	1.29	1.39	1.49	1.59

PDMS rubbers were created by mixing 1.82 g of the base (siloxane oligomer) and 0.18 g of the curing agent (siloxane crosslinker) from the Sylgard®184 kit, before placement in a vacuum for 24 h to facilitate curing. These elastomers along with poly-ACR and poly-HEMA served as controls for all ensuring experiments. For each type of polymer and control, a 0.635 mm punching tool was used to obtain circular coupons [Figure 5].

Figure 5: Copolymer coupons obtained using a 0.635 mm punching tool once the solid elastomers had been synthesized, soaked in propanol for 12 h and dried for 48 h.

2.2.3. Material Characterization

2.2.3.1. Light Transmittance

Coupons of the copolymers and controls (n = 6 for each type) were placed in a 96-well Greiner transparent flat-bottom plate, and light transmittance readings over the range of visible wavelengths (400- 750 nm) at intervals of 10 nm were obtained from a SpectraMac®Plus^{384} Absorbance Microplate Reader at room temperature.

2.2.3.2. Surface Roughness

Atomic Force Microscopy (AFM) micrographs were obtained using a Digital Instruments NanoScope IIIa Multimode scanning probe microscope (Veeco) for each copolymer and PDMS. The instrument was operated in tapping mode using an Olympus

silicon tapping probe (tip radius, <10 nm) operated at a 1.0 Hz scan rate over a 1 µm x 1 µm scan area. Given the small scan area, triplicate measurements for each type of polymer were obtained from different areas from the surface of one coupon. Representative images are shown in Figure 7.

2.2.3.3. Shore Hardness

Copolymer stiffness was measured by stacking coupons to a height ≥ 6 mm and measuring the resistance to indentation of the topmost disc using a standard dial Shore 00 Rex durometer (Model 1600, error ± 5 durometer points). The durometer was held in a near-vertical position while the foot of the gauge was allowed to press into the specimen from the weight of the instrument. The reading on the durometer at the start and end of 10 s of firm contact was recorded. The two readings ensured any ‘creep’ of the dial hand to lower values was captured. The process was repeated for 6 different coupons of each polymer type to get an average hardness for each [Figure 8].

2.2.3.4. Water Uptake and Surface Wettability

The average (n = 6) water uptake for each polymer type was measured by recording the weight of each coupon before and after immersion in dH_2O for 30 min. The percent weight gain was calculated and plotted [Figure 9]. The contact angles for similarly hydrated coupons were obtained via the captive bubble technique and a conventional goniometer microscope. Copolymer discs were individually inverted and submerged in a cuvette filled with Milli-Q (18 MΩ/cm) H_2O, and an inverted micrometer syringe with a curved needle was used to introduce ~15 µL of air onto the center of the polymer. The angle formed at the air/solid interface in the aqueous environment was recorded. Results are presented as an average of contact angles for 6 different coupons of each copolymer type.

The static sessile-drop method was used to obtain contact angles for dry copolymers and controls using a Ramé-Hart NRL C.A. goniometer (Mountain Lakes, NJ). Approximately 0.02 mL of Milli-Q water was introduced to the center of each coupon surface and the drop profile was photographed at 0, 30, 60, 120 and 180 s after contact using the Krüss Drop Shape Analysis software (v.10). GIMP2 Image Analysis Software was subsequently used to measure the internal contact angles (between the drop and the solid surface) on either side of the drop in an image and values were averaged to provide the contact angle for that photo. The procedure was repeated for the images of all polymers (n = 6 for each type) at 0 and 180 s. Average static sessile drop contact angles were plotted for comparison between polymers [Figure 12].

Energy Dispersive X-Ray (SEM-EDX) was performed for elemental analysis on the surfaces and cross-sections of all copolymers using a Tescan, VEGA-LSU SEM. Select images are provided in Figure 13.

2.2.4. Bacterial Toxicity Assays

LB agar plates were created using 10 g of tryptone, 5 g of yeast extract, 10 g of NaCl, 15 g of agar and 1 L of distilled water (dH_2O). The dry ingredients were measured into a 2 L Erlenmeyer flask followed by 500 mL of dH_2O and the mixture was stirred to achieve complete solvation of the starting materials. The agar was added along with the rest of the H_2O before the solution was autoclaved. Following autoclaving, approximately 12 mL of the media were transferred into a dish in a laminar flow hood and the process was continued until all the media had been utilized. The media in the dishes was left to solidify for 30 min, after which the capped plates were stacked in their original packaging, sealed and stored at 4 °C until further use. LB media for culturing *E. coli* in solution was made in the same manner with the exception of agar. The autoclaved solution was sealed and stored at room temperature.

The IPTG-inducible, GFP-producing K-12 strain of *E. coli* obtained from the Promega Corporation was used to create a stock and working *E. coli* solution. 100 µL of *E. coli* solution was streaked onto an agar plate that was incubated at 37 °C overnight. A single colony from the plate was transferred into 10 mL of LB media using an autoclaved pipette tip. After another overnight period of incubation, 100 µL of the solution was added to a fresh vial containing 10 mL of LB media. This second vial was incubated overnight and stored at 4 °C as the working solution until further use and for a maximum

of 1 week. To the first vial, 10 mL of autoclaved glycerol were added and the stock mixture was stored at -80 °C. Glycerol serves as a cryoprotective agent that mitigates the risk of ice crystal formation and subsequent damage to cultured cells.[45]

To run the antibacterial assay, 100 µL of the working solution were aseptically spread onto a pre-made LB agar plate using a sterilized cotton swab. The agar surface was allowed 5 min to dry and then autoclaved forceps were used to gently but firmly press the 60 wt% ACR copolymer coupons onto the surface. The process was repeated to create an agar plate for each of the PDMS, 70 wt% ACR and 80 wt% ACR copolymers. Two drops each of the ACR and deinhibited HEMA monomer were added to precut filter papers, which were then pressed onto their respective plates. The entire set was incubated overnight at 37 °C and the results were photographed [Figure 6].

2.2.5. Leachates

All polymers (n = 1 for each type) were synthesized and placed in specimen jars containing 40 mL of 2-propanol for 12 h as described earlier. Each jar was capped to prevent solvent evaporation during the course of the study. 1 mL aliquots of the 2-propanol were obtained at 5, 10, 15, 20, 25, 30 (0.5h), 60 (1 h), 90 (1.5h), 120 (2 h), 150 (2.5 h), 180 (3 h), 240 (4 h), 300 (5 h), 360 (6 h), 540 (9 h), 700 (12 h) min, respectively, from the start of the extraction process for each of 60, 65, 70, 75 and 80 wt% ACR copolymers. Aliquots obtained at 10, 20 and 30 min were selected for analysis and the 2-propanol in each of these vials was removed by evaporation under reduced pressure. Upon complete evaporation, 1 mL of deuterated chloroform and 5 µL of *tert*-butanol were added to each of the vials, the entire contents of which were then transferred into NMR

tubes and submitted for analysis. ^{1}H NMR spectra were recorded for all samples at room temperature using a Bruker AV-500 (at 500.13 MHz) and the peak for deuterated chloroform was set at 7.26 ppm. Spectra for HEMA, ACR, DMPA and DEGDA were used as controls, while the peaks on those for the copolymers were integrated relative to tert-butanol (set as 9 protons). The relative values for ACR and HEMA at 10 and 20 min were listed in Table 2.

2.2.6. *Escherichia coli* (*E. coli*) Adhesion Studies

The protocol for the adhesion assay was based on published results[46,47,48] 100 µL of *E. coli* culture broth were streaked on an agar plate that was incubated overnight. Multiple colonies (3-4) were obtained from the resultant lawn using an autoclaved pipette tip and a new vial of broth (200 mL) was inoculated. This vial was placed in an incubator from where 1 mL aliquots were taken every 30 min to measure the OD_{600} of the solution. Once the OD_{600} value reached 0.7, 0.5-1 mM, IPTG was added to the vial, which was incubated for 5-6 h. *E. coli* from the vial was filtered using a cellulose acetate filter 0.45 microns (37 mm diameter) and the filter paper was washed thrice with autoclaved 0.9% PBS into new vial. 100 mL of PBS were added to the vial, which was supplemented with 2% w/v nutrient broth. The solution was agitated to facilitate equal dispersion of *E. coli*. Copolymer coupons (n = 4 for each type) were placed in a 48- well polystyrene, flat-bottom plate and to each polymer-containing well, 400 µL of the broth-supplemented *E. coli* mixture were added. The plate was incubated overnight (12 h), after which each coupon was removed from its well using sterile forceps, rinsed thrice with autoclaved PBS and placed in a well of a fresh plate. A microplate reader (Gemini XPS) was used to

obtain GFP fluorescence readings using an excitation and emission wavelength of 395 nm and 509 nm, respectively, from the rinsed polymer coupons in the new plate. The procedure was repeated for hydrated coupons (coupons that had been soaked in dH_2O for 30 min prior to incubation with 400 µL of broth-supplemented *E. coli* in PBS). The fluorescence readings for each set were plotted for comparison after the background fluorescence (reading from a sample of each type incubated with uninduced *E. coli*) had been subtracted. Readings for the dry set were also plotted against the average percent water uptake and the sessile drop contact angles to determine the correlation, if any, between the three different variables.

2.2.7. Preliminary Human Corneal Epithelial Cell (HCEC) Study

Frozen stocks of low-passage (7- 9) HCECs at -80 ^{o}C were provided by the Sheardown lab at McMaster University. Keratinocyte serum-free medium (KSFM) supplemented with prequalified human recombinant Epidermal Growth Factor 1-53 (EGF-153) and Bovine Pituitary Extract (BPE) was obtained from Gibco. Penicillin-streptomycin (Invitrogen, Carlsbad, CA, USA) was added to the KSFM (1%) to prevent bacterial contamination.

A stored cryovial was thawed and the contents (1mL) were transferred into a Falcon tube containing ~6.5 mL of media containing serum (25 mg/mL). The tube was centrifuged at 900 rpm for 5 min to remove the dimethylsulfoxide (DMSO) cryoprotective agent as part of the supernatant. Fresh serum-containing media (7 mL) was used to gently resuspend the HCEC pellet and the mixture was transferred into a 25 cm^2 culture flask that was incubated at 37 °C and 5% carbon dioxide (CO_2). Every 2-3 days

the solution in the flask was aspirated and replaced with fresh 6.5 mL of media with serum until ~80% confluency of cells was achieved. The liquid from the flask was subsequently aspirated and the HCECs were gently rinsed with 5 mL of sterilized PBS to remove dead cells. Aspiration of the buffer was followed by addition of 1 mL of TrypLE^{TM} Express from Invitrogen and an incubation time of ~5-10 min. Care was taken to remove the flask from the incubator exactly at the conclusion of time, since prolonged exposure to the trypsin in the reagent could damage cells. To mitigate this, 4 mL of sterile PBS was mixed with the TrypLE^{TM} Express and the solution was transferred into a falcon tube for centrifugation at 900 rpm for 5 min. Most of the supernatant was subsequently discarded and the pellet was gently resuspended in what little remained of the solution from the last step. Of this, 10 µL was placed in a hemocytometer and the amount of media required to ensure 35 µL of the final cell suspension contained 10,000 cells was calculated using the following equation:

$$\frac{\text{Number of Cells Counted}}{\text{4 Grids}} \times \frac{1}{\text{Depth of Grid (0.1mm)}} \times \frac{1}{\text{Surface area of Grid (1mm}^2} = \frac{\text{Amount of Cells}}{\text{mm}^3}$$

Consequently, ~5.2 mL of KSFM were added to the tube in preparation for the seeding of the copolymer surfaces.

Three coupons each of PDMS and 60- 80 wt% ACR copolymers, total 24 samples, were placed in a 48- well plate and incubated with KSFM supplemented with 1% penicillin-streptomycin for 24 h. At the end of time, media from each coupon-

containing well was removed and 35 µL of the cell suspension was placed on each of the surfaces. The plate was covered and incubated for 20-30 min to allow for cell adhesion and then 200 µL of KSFM were added to each well to submerge the samples. The plate was placed back in the incubator and the KSFM was replaced every on the second day prior to photographing the surfaces with a Zeiss Axiovert 200 Microscope using a 10x objective. The optical images thus obtained are seen in Figure 21.

2.3. Results

2.3.1. Polymer Preparation

Copolymers of HEMA and a novel silicone surfactant (ACR) were synthesized via radical polymerization for 30 minutes in a N_2- rich atmosphere. The constituent monomers were varied by weight percentages to afford polymers with 60-80 wt% ACR, which were subsequently soaked in 2-propanol for 12 hours. After 48 hours of drying, a 0.635 mm punching tool was used to obtain the circular coupons.

Qualitatively, it seemed that the copolymer stiffness increased with decreasing weight percent ACR, thus coupons from copolymers with higher weight percentages of ACR were easier to extract. The exception was poly-ACR that ‘crumbled’ upon firm contact making the removal of circular coupons of equal sizes difficult. Though higher weight percentages of ACR (70- 80 wt%) facilitated the removal of coupons, they also increased the likelihood of surface grooves during polymerization and surface artifacts during coupon extraction. Copolymers containing 65 - 80 wt% ACR were optically transparent whereas the 60 wt% ACR copolymer appeared cloudy.

2.3.2. Polymer Characterization

2.3.2.1. Light Transmittance

Average light transmittance values for copolymers were obtained using a standard microplate reader. Copolymers of 70, 75 and 80 wt% ACR exhibited transmittance values >80%, while poly-HEMA and 60 wt% ACR had substantially lower values (~50%). Poly-ACR and 65 wt% copolymers transmitted ~70% of the incident light. Interestingly, the transmittance values for each polymer except PDMS increased between the wavelengths of ~400-450 nm before reaching a plateau. The values for PDMS do not seem to exhibit this phenomenon.

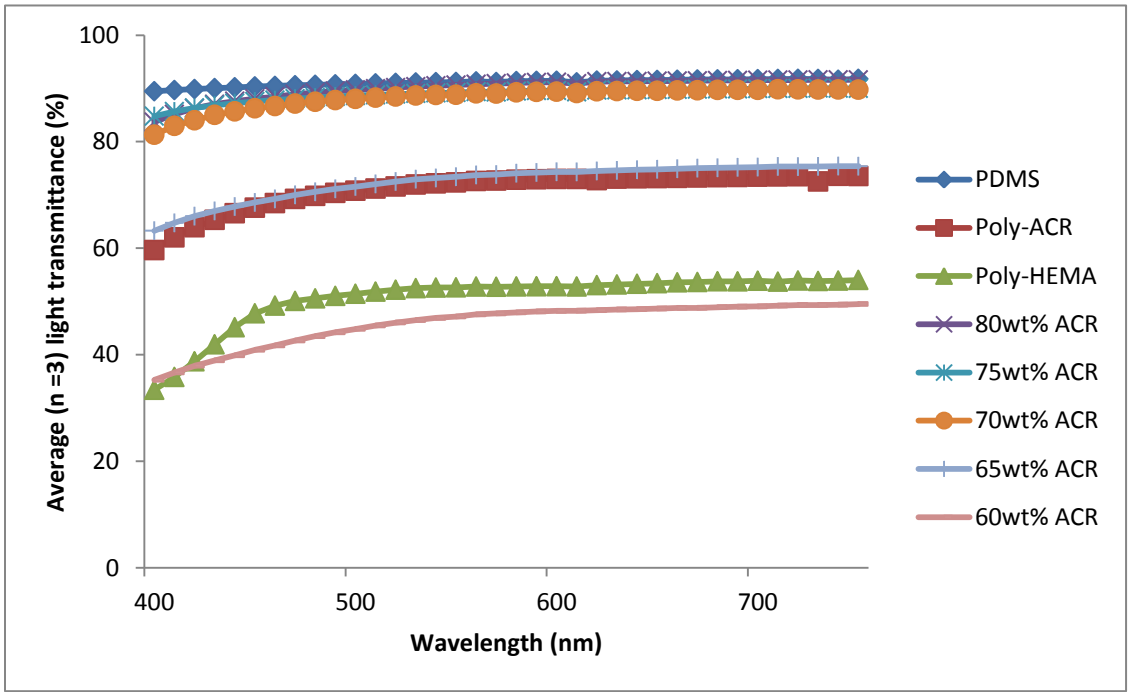

Figure 6: Percent light transmittance for copolymers and controls over the range of visible wavelengths (400-750 nm).

2.3.2.2. Surface Roughness

The roughness in a 1 µm x 1 µm site was measured for each synthesized copolymer and found to be comparable to PDMS: all were very flat, exhibiting surface roughnesses in the 2-3 nm range. Two other 1 µm x 1 µm sites were selected on the surfaces to achieve triplicate measurements for each copolymer, and the surface roughness result was the same in each case. The streaking that is sometimes visible in the micrograph for 75 wt% ACR is attributable to the drag and drift of the AFM cantilever tip over the coupon surface.

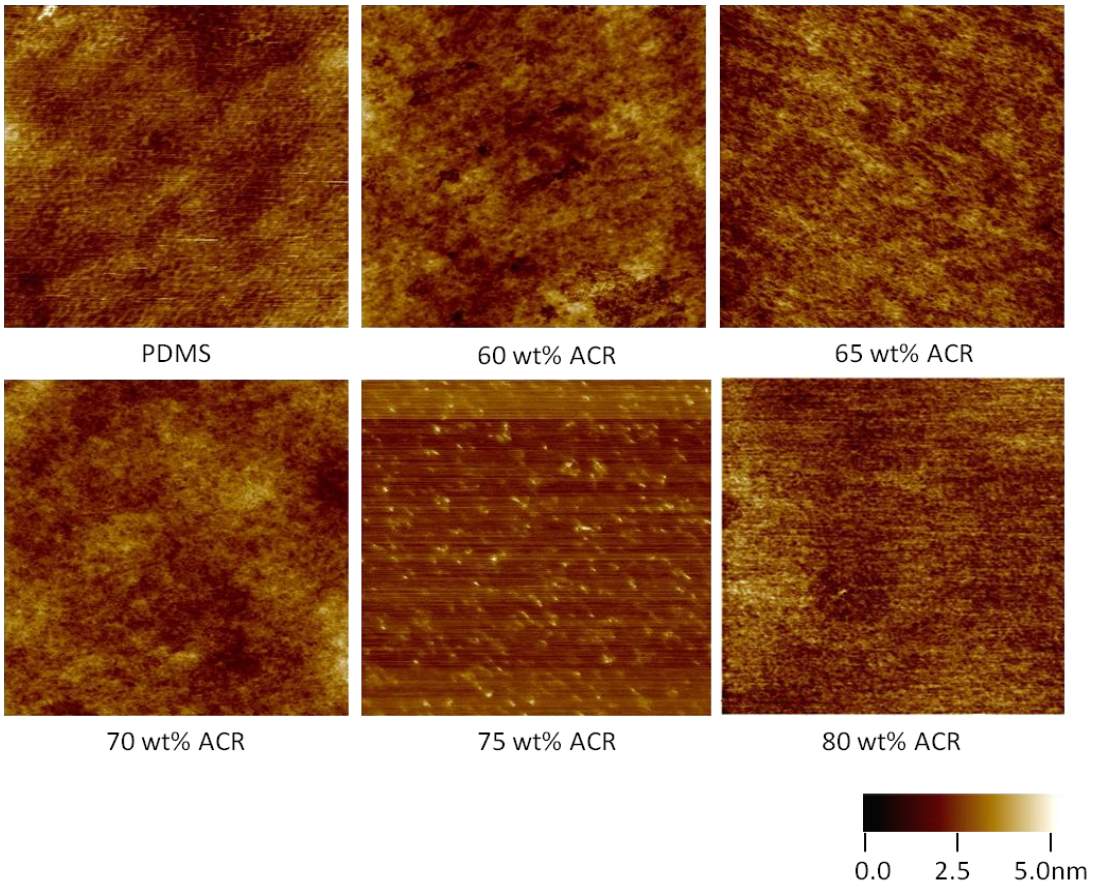

Figure 7: AFM micrographs for the copolymers (60- 80 wt% ACR) and PDMS.

2.3.2.1. Shore Hardness

A Rex durometer was used to determine the hardness values of copolymers and the readings before and after ten seconds of contact were recorded. No creep was observed and the average readings from 6 coupons of each polymer type ranged from 78-93 hardness points- (creep 0 at 10sec, 24 °C)- for poly-ACR and 65 wt% ACR copolymers respectively. Hardness values seemed consistent across the copolymer series and highly comparable to the hardness of PDMS.

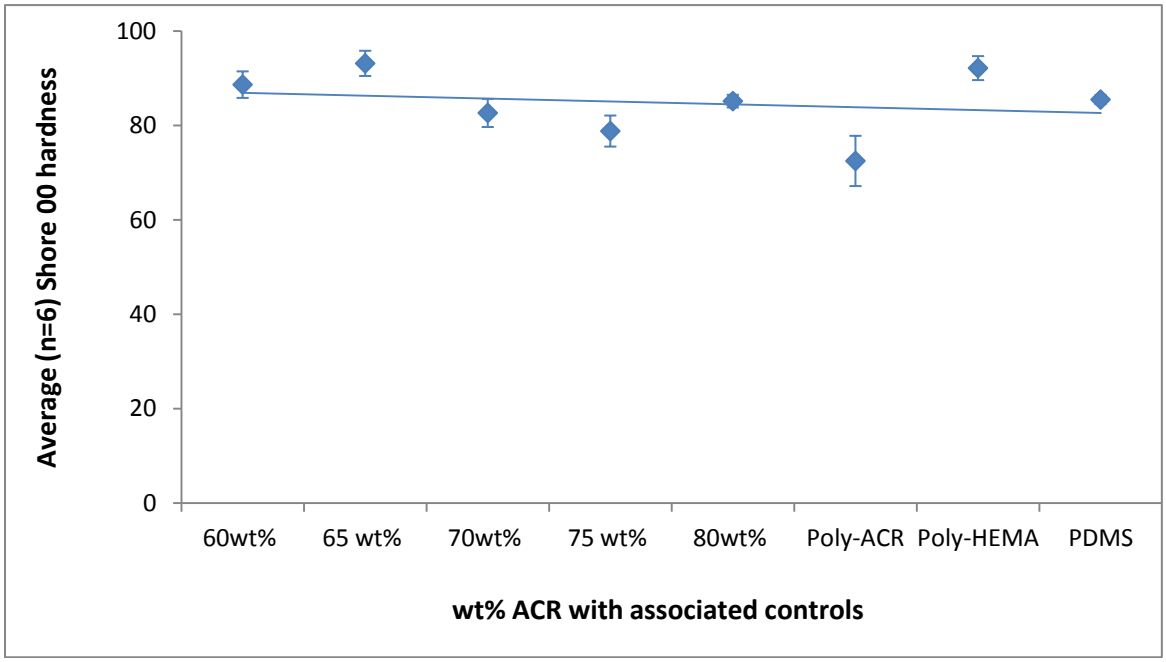

Figure 8: Shore 00 hardness values for the copolymer series and controls.

2.3.2.1. Surface Wettability

The average percent water uptake for 6 coupons of each polymer was obtained by measuring the weight of coupons before and after immersion in dH_2O for 30 minutes. If

viewed in the absence of error bars, the data suggests increasing percent uptake with increasing wt% ACR to a maximum point, since the highest water uptake (43.98%) was seen with the 75 wt% ACR copolymer and much lower uptake values were seen for Poly-ACR and the 80 wt% ACR copolymers (20.52% and 23.68% respectively). The overlapping error bars, however, make it difficult to discern a definitive trend. PDMS exhibited an 8% water uptake, which was the lowest uptake value of the group.

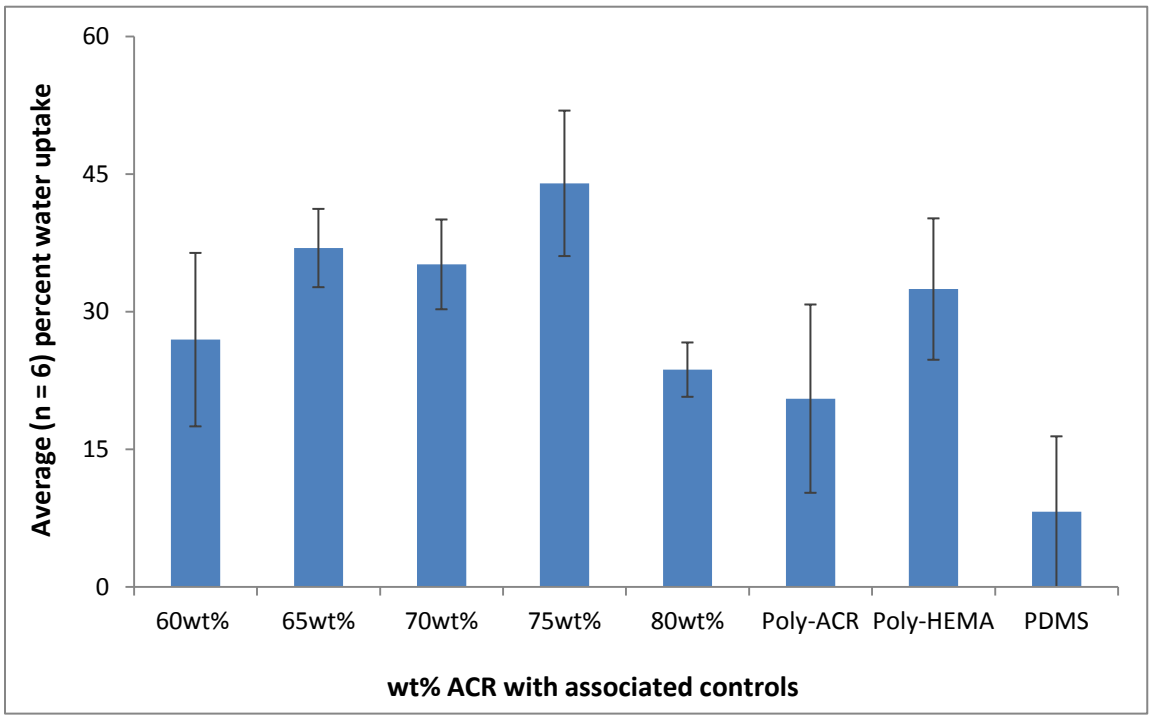

Figure 9: Average (n = 6) percent water uptake of copolymers and controls.

An interesting qualitative observation during the water uptake study was the increase in tackiness of hydrated coupons vs. the non-hydrated counterparts. When removed from water, blotted with a KimWipe and placed on weighing boats, hydrated coupons adhered to the bottoms [Figure 11.a] and were difficult to remove even via

careful peeling with tweezers. This tackiness seemed more apparent in copolymers of higher ACR weight percentages. Furthermore, bubbles formed along the copolymer surfaces during immersion of the materials in water. Whereas for the copolymers the bubbles were situated along the edges of the coupons [Figure 11.b], they were only visualized on the upper and lower surfaces of the poly-ACR disks.

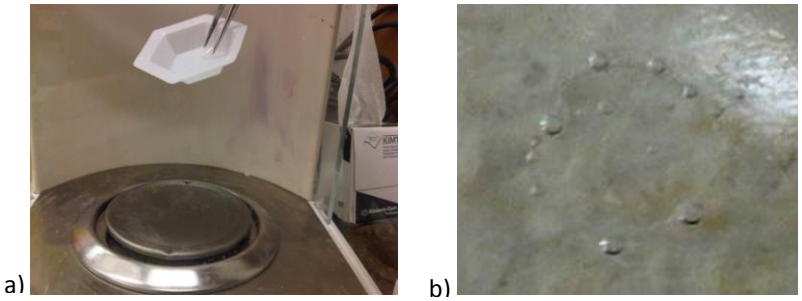

Figure 10: Qualitative observations of a) tackiness and b) bubble formation for the 25 wt% ACR copolymer during the percent water uptake study.

The hydrated coupons were then inverted and submerged in a Milli-Q water-filled chamber where an air bubble was introduced to the coupon surface using an inverted micrometer syringe. The captive bubble contact angles were calculated manually using a standard goniometer microscope. As with the Shore 00 hardness data for the series, the contact angles were consistent despite changes in the bulk composition of coupons [Figure 11] with the mean contact angle for the set being 30° (± 3.2°).

Contact angles for a dry polymer set were also obtained. Using the static sessile-drop method, drop profiles on the surfaces of 6 disks of each polymer type at multiple time points were photographed using Drop Shape Analysis software on a standard

goniometer. The angles from the images were measured using the GIMP2 Image Analysis Software. Average sessile drop contact angles at 0 and 180 seconds were plotted to yield Figure 12.

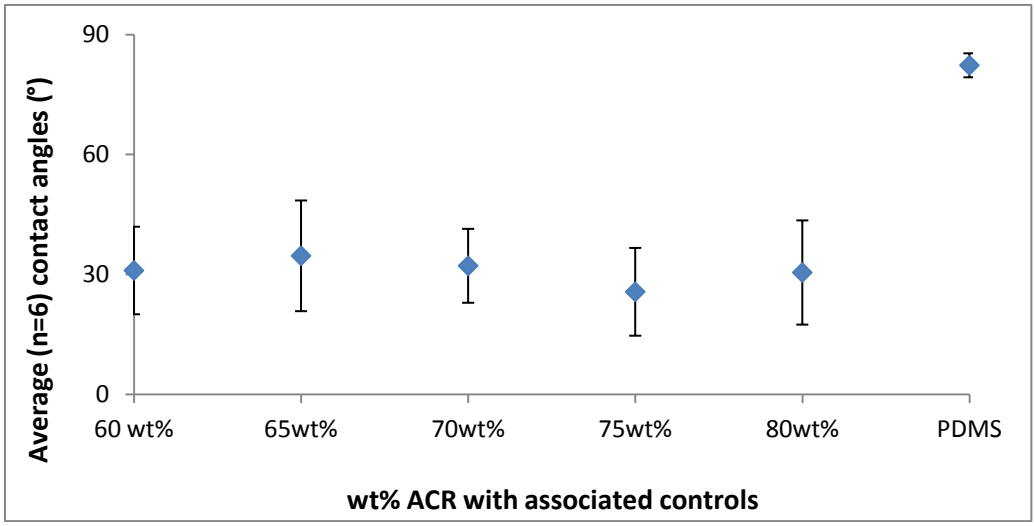

Figure 11: Average (n = 6) captive bubble contact angles for hydrated copolymers and PDMS.

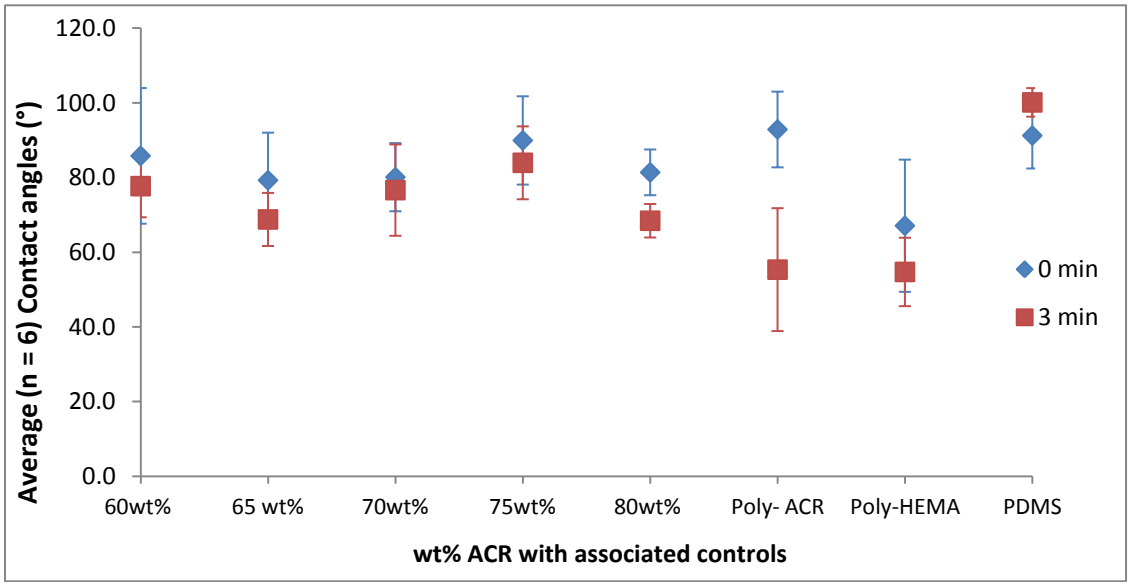

Figure 12: Average (n = 6) sessile- drop contact angles for dry copolymers and controls at 0 and 180 s.

Again, no variation in contact angles between the copolymers was observed. The angles obtained for the copolymers at 0 seconds were highly comparable to PDMS (mean angles for copolymer series and PDMS were ~81° and 91.2°, respectively with paired $t(7) = 2.2$, $p = 0.06$). In light of the percent water uptake results, the tight similarity between contact angles at 0 and 180 seconds for the copolymers is surprising. Differences in angles obtained at the two time points become apparent with the 80 wt% ACR copolymer and especially poly-ACR. The contact angle for PDMS seems to increase from 91.2° to 100.1° after 3 minutes of time.

To test the hypothesis of surface homogeneity across the copolymer series, a Tescan, VEGA-LSU SEM was used to perform Energy Dispersive X-Ray (SEM-EDX) analysis on the surfaces and cross-sections of the coupons [Figure 13].

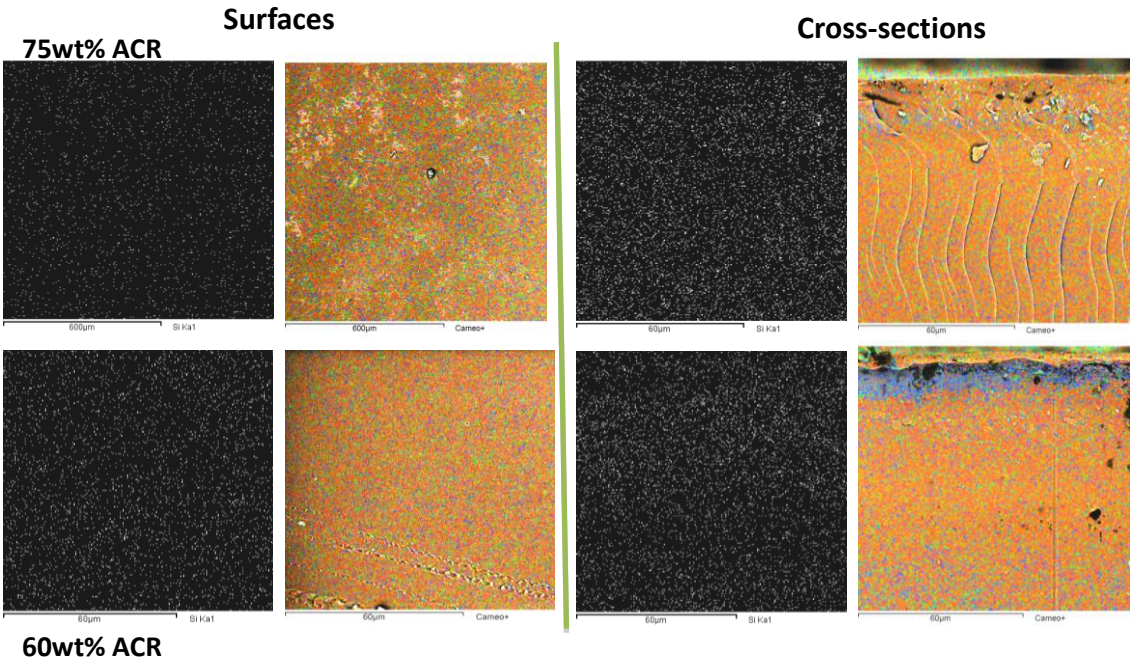

Figure 13: Elemental analysis for silicon on the surfaces and cross-sections of the 60 wt% ACR and 75 wt% ACR copolymers.

Since each image yielded similar results, only the pictures for the 60 wt% ACR and 75 wt% ACR copolymers are shown. The silicon appeared to be equally dispersed throughout the entire system.

2.3.3. Antibacterial Activity of ACR

A modified adaptation of the Kirby-Bauer test formed the basis of the antibacterial assay. Briefly, 100 µL each of an *E. coli* working solution were aseptically spread onto 5 pre-made sterile LB agar plates. Coupons of the polymers were pressed firmly onto the agar surface and incubated with the plate overnight for 12 hours at 37 °C. The procedure was repeated with precut filter papers to which two drops each of the HEMA and ACR monomers had been added.

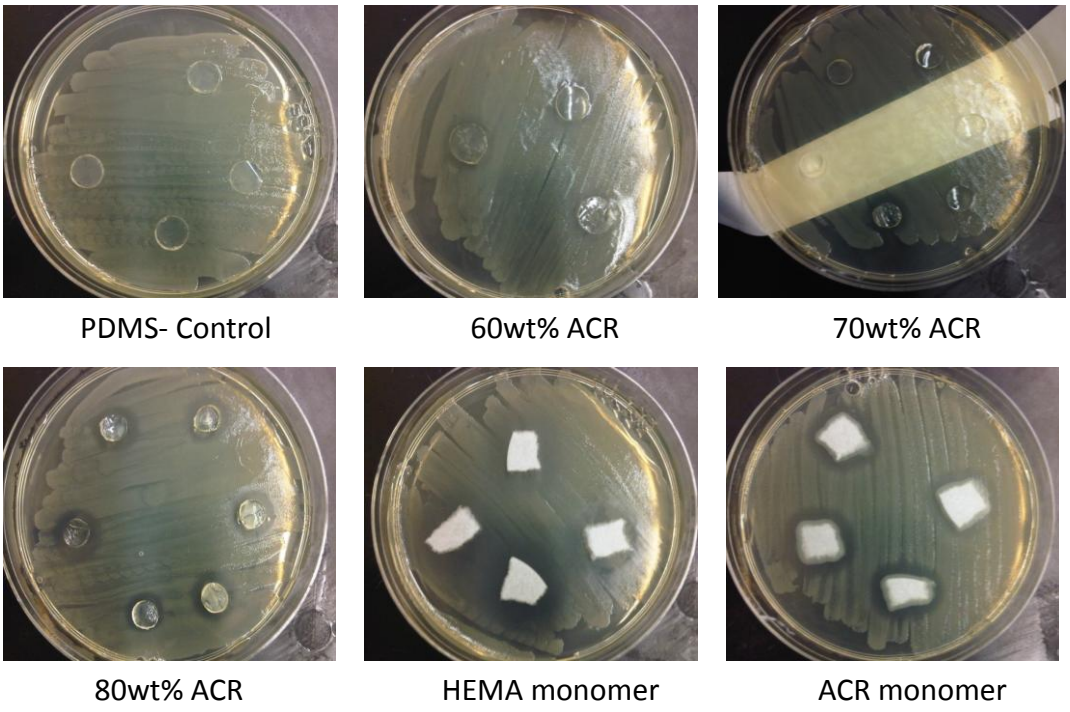

Figure 14: Zones of inhibition (ZOIs) produced by the 60, 70 and 80 wt% ACR copolymers and the ACR and HEMA monomers.

Clear zones of inhibition (areas devoid of bacterial growth) were seen around 60, 70 and 80 wt% ACR copolymers and the ACR and HEMA monomers [Figure 14]. Qualitative comparison indicated seemingly larger zones of inhibition around copolymers with higher weight percentages of ACR.

The antibacterial assay was re-run using coupons from copolymers that had been soaked in 40 mL of 2-propanol for 12 hours prior to drying and disk extraction. No ZOIs were visible on the agar surfaces around or underneath the specimens [Figure 15].

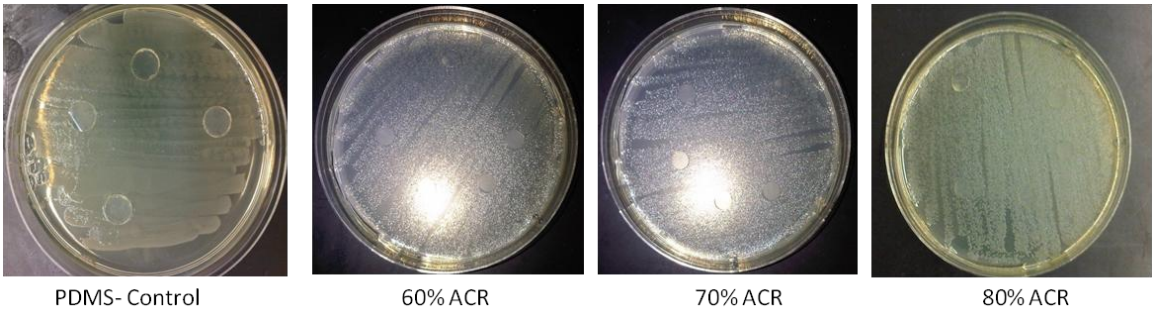

Figure 15: Absence of zones of inhibition (ZOIs) around and underneath extracted copolymers.

It seemed that a considerable portion of the product was being lost during the extraction process. To quantify this observation, the weight percent decrease for copolymers after 12 hours of extraction and 24 hours of drying was calculated and plotted [Figure 16]. The greatest loss in weight (~45%) was seen in the 80 wt% copolymer followed by poly-ACR at ~40%. Poly-HEMA showed the least drop in weight (<5%) while the weight loss appeared to correlate positively with increasing wt% of ACR. Given

the significant decrease in weight after extraction, a more thorough NMR study of the leachates was conducted.

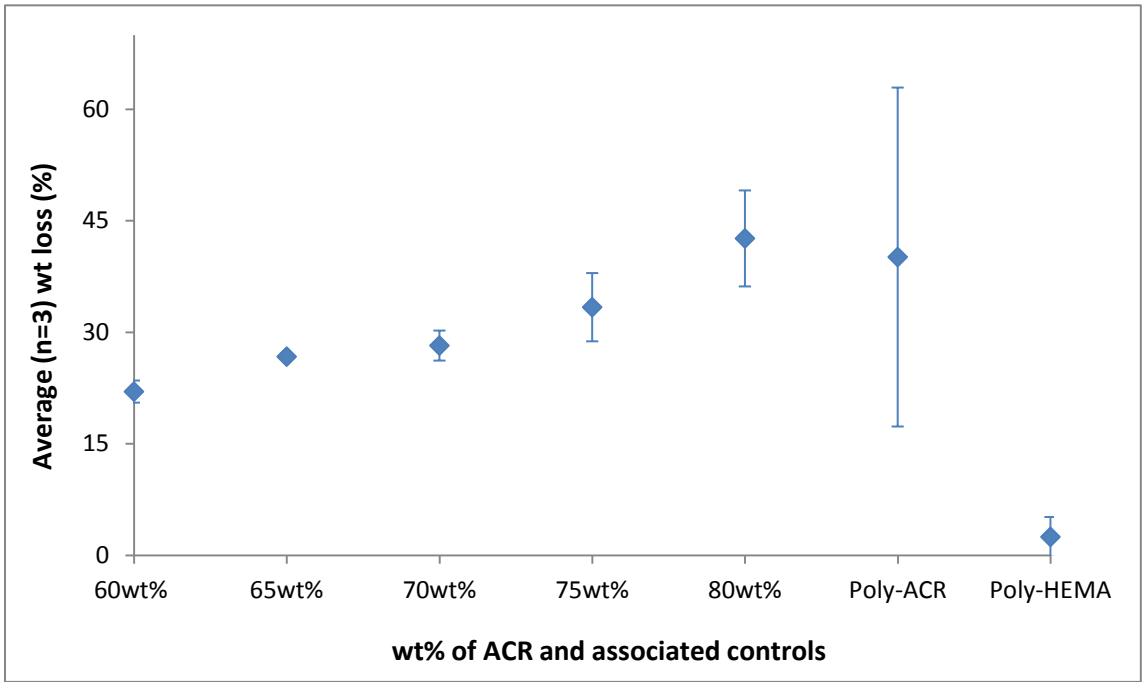

Figure 16: Average (n = 3) weight percent loss of copolymers after 12 hours of extraction in 2-propanol and 24 hours of drying.

2.3.4. Issues with Extractables

Initially it was thought that the drop in mass after extraction indicated insufficient time for complete polymerization of reagents. Since a small film of liquid was always observed on the surface of the solid polymer after 30 minutes of curing, this assumption seemed reasonable. Longer curing times were tried, but the film of liquid could not be eliminated. Consequently, it was hypothesized that one or more of the reagents was in excess and an NMR study was designed to confirm the identity of the leachants, quantify

the relative amounts of each, and to ascertain the optimal extraction time by comparing the amount of leachants in the solvent at different time points.

After synthesis, copolymers were placed in capped specimen jars containing 40 mL of 2-propanol for 12 hours. 1 mL aliquots were removed from the jars at various time-points but only those obtained at 10, 20 and 30 minutes were used in subsequent steps. The propanol from these samples was evaporated, and deuterated chloroform and tert-butanol were added prior to submission for ^{1}H NMR analysis. According to the table of integration values relative to that of tert-butanol [Table], ACR appears to be the primary leachate since it has higher values than HEMA at all time-points, and since the relative amount of ACR leached increases with copolymers of increasing weight percent ACR.

Table 2: Integration values of ACR and HEMA relative to tert-butanol, which was calibrated as 9 protons.

		Leachate	
Polymer type	**Time points**	**ACR**	**HEMA**
60 wt% ACR	10 min	1.9088	0.1871
	20 min	2.6965	0.2854
65 wt% ACR	10 min	1.931	0.1786
	20 min	2.5634	0.2368
70 wt% ACR	10 min	1.868	0.0603
	20 min	1.2848	0.0756
75 wt% ACR	10 min	2.8635	0.1642
	20 min		
80 wt% ACR	10 min	2.9993	0.1005
	20 min	3.2638	0.1056

2.3.5. *Escherichia coli* (*E. coli*) Adhesion Study

The protocol for this assay was adapted from multiple sources. Briefly, coupons obtained from leachate-free copolymers were incubated with equal volumes of *E. coli* in PBS. The coupons were subsequently rinsed with sterilized PBS and placed in a fresh 48-well flat bottom plate. GFP fluorescence readings from the surfaces of coupons were measured using a microplate reader. The plotted data [Figure 17] showed no difference in relative fluorescence and therefore adhesion across the copolymer series. Despite the overlap in error bars, the poly-ACR appears to have a higher fluorescence value (7629 RFUs) than the other polymers in the set (mean fluorescence ~3085.4 RFUs).

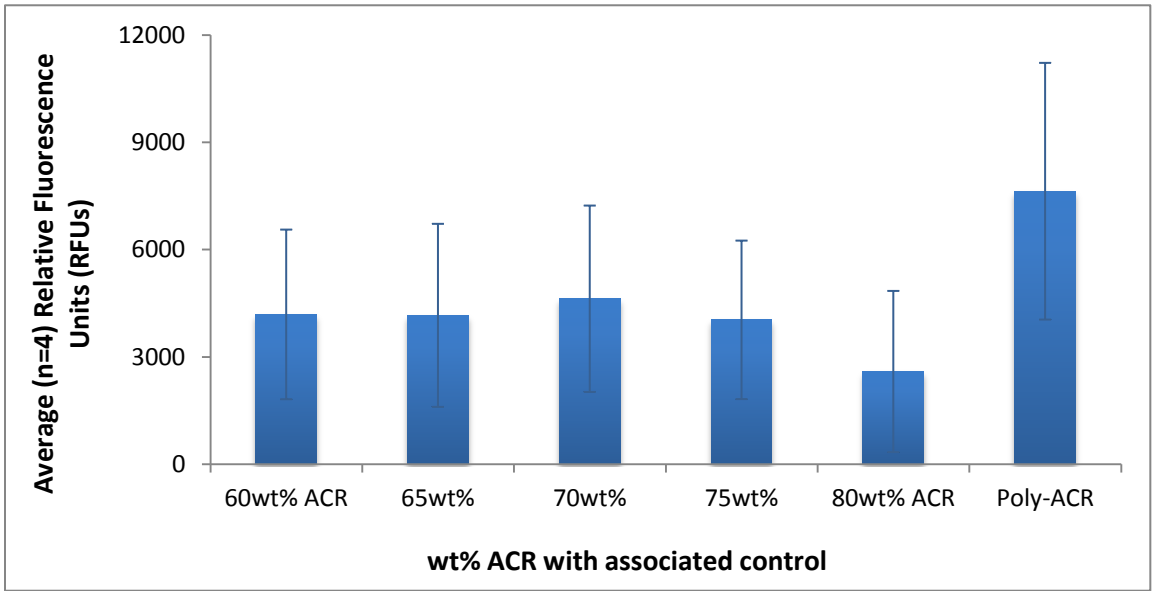

Figure 17: Average (n = 4) relative GFP fluorescence readings from IPTG-induced *Escherichia coli* adhered to copolymer surfaces and control.

Given the absence of two controls (PDMS and poly-HEMA), and the fact that copolymers were shown to absorb water, the experiment was repeated with dry and

hydrated copolymers, respectively, that had been immersed in dH_2O for 30 minutes prior to use in the assay, to determine the difference in *E. coli* adhesion between the two sets.

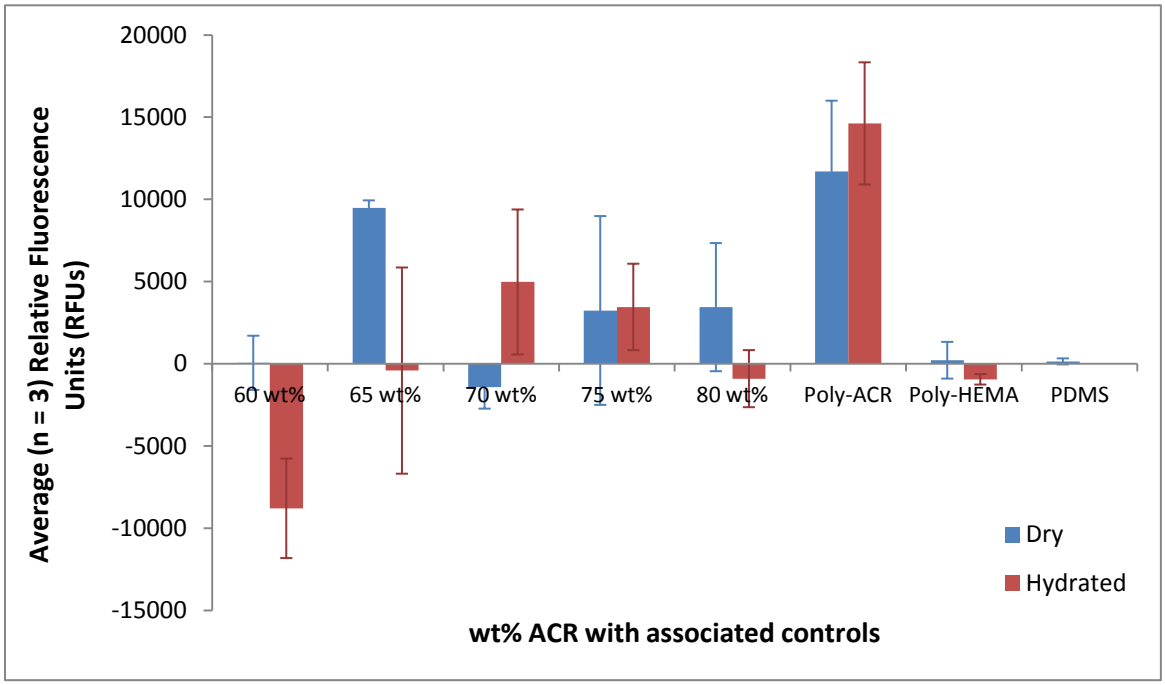

Figure 18: Average (n = 3) GFP fluorescence readings from IPTG-induced *Escherichia coli* adhered to dry and hydrated copolymer surfaces and controls.

Unlike the first run, the repeat of the experiment did not yield consistent readings across either copolymer set. No discernible trend was evident. Negative fluorescence values were seen for 60, 65, 80 wt% ACR copolymers in the hydrated series and the 70 wt% ACR copolymer from the dry ones. Interestingly poly-ACR again had the highest fluorescence (11,693 RFUs), which increased for the hydrated coupons to ~14,616 RFUs. The fluorescence data from the first adhesion experiment was plotted against the sessile-drop contact angles [Figure 19] to determine the correlation (if any) between *E. coli* adhesion and surface wettability for these ACR-HEMA copolymers. The gradient to the

regression suggested a positive correlation between the two variables while the coefficient of determination (R^2) was 0.423.

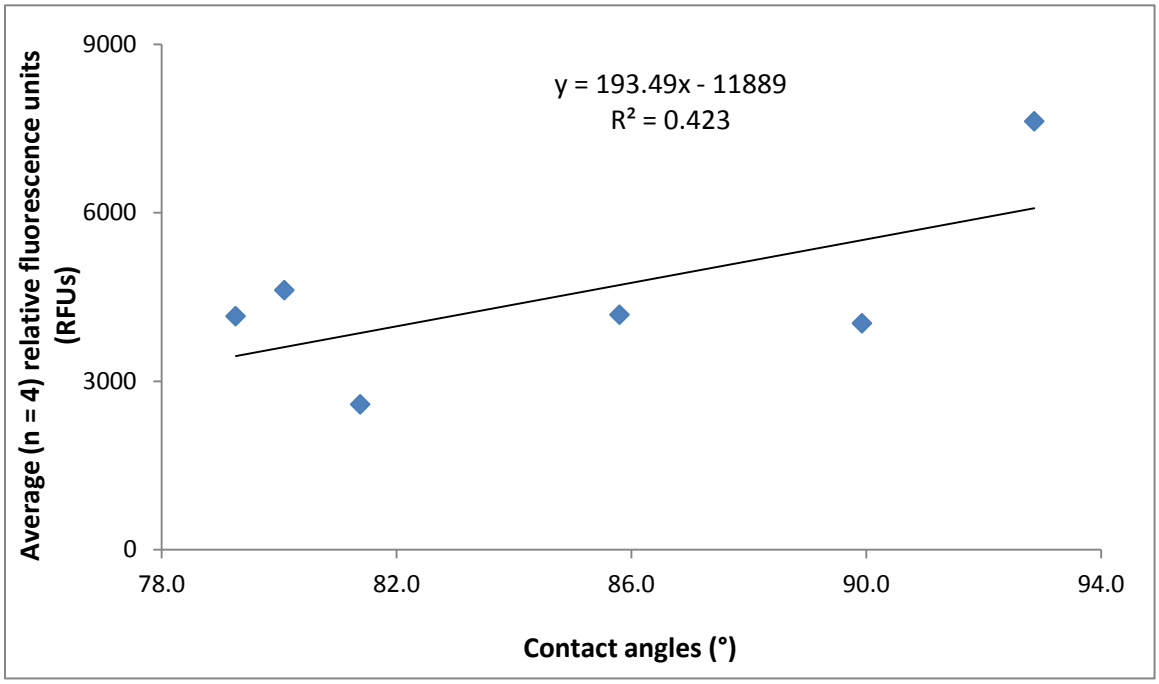

Figure 19: Average (n = 4) GFP fluorescence readings vs. the average (n = 6) sessile-drop contact angles for the dry ACR-HEMA copolymers.

The first set of fluorescence data was also plotted against the average percent water uptake [Figure 20] for the dry copolymers. A negative correlation between the two parameters was observed with a coefficient of determination (R^2) lower than that for fluorescence vs. contact angles (0.1138 and 0.423, respectively).

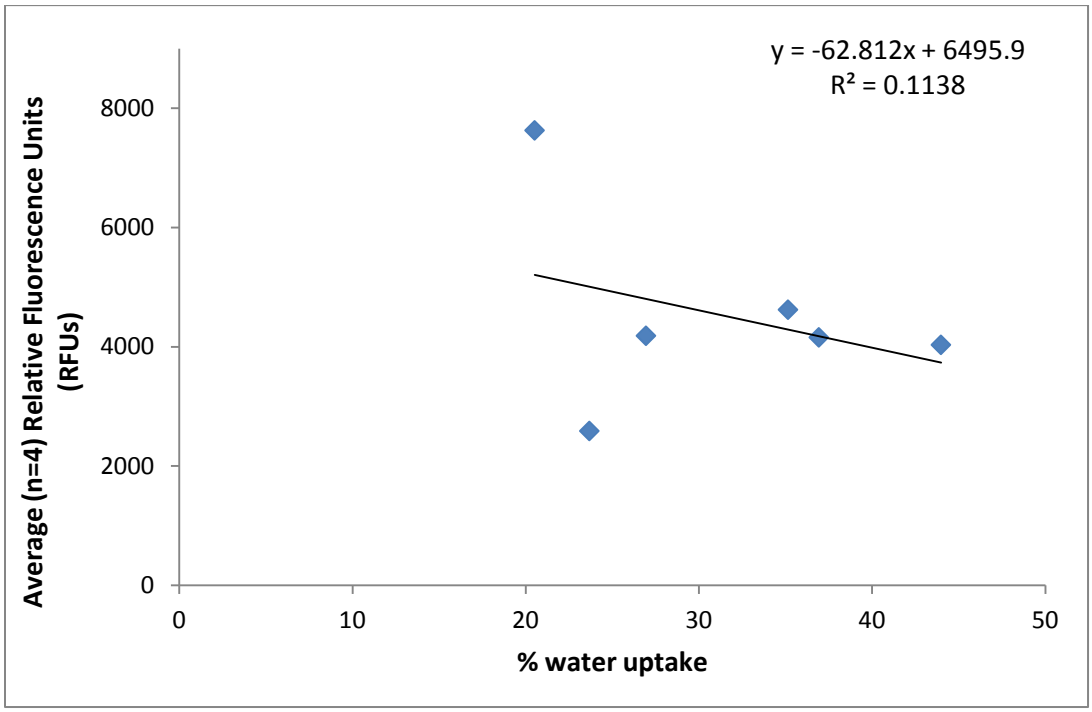

Figure 20: Average (n = 4) GFP fluorescence readings vs. the average (n = 6) percent water uptake for the dry ACR-HEMA copolymers.

2.3.6. Preliminary Human Corneal Epithelial Cell (HCEC) Compatibility Study

Low passage HCECs were cultured in serum-containing media then resuspended in keratinocyte serum-free medium (KSFM). In the interim, copolymer coupons were incubated with KSFM and penicillin-streptomycin for 24 hours. At the conclusion of time and once the coupons had been placed in a fresh 48-well polystyrene plate, the surfaces were seeded with HCECs and the plate was incubated. Two days after seeding, a camera-fitted optical microscope was used to photograph the surfaces [Figure 21].

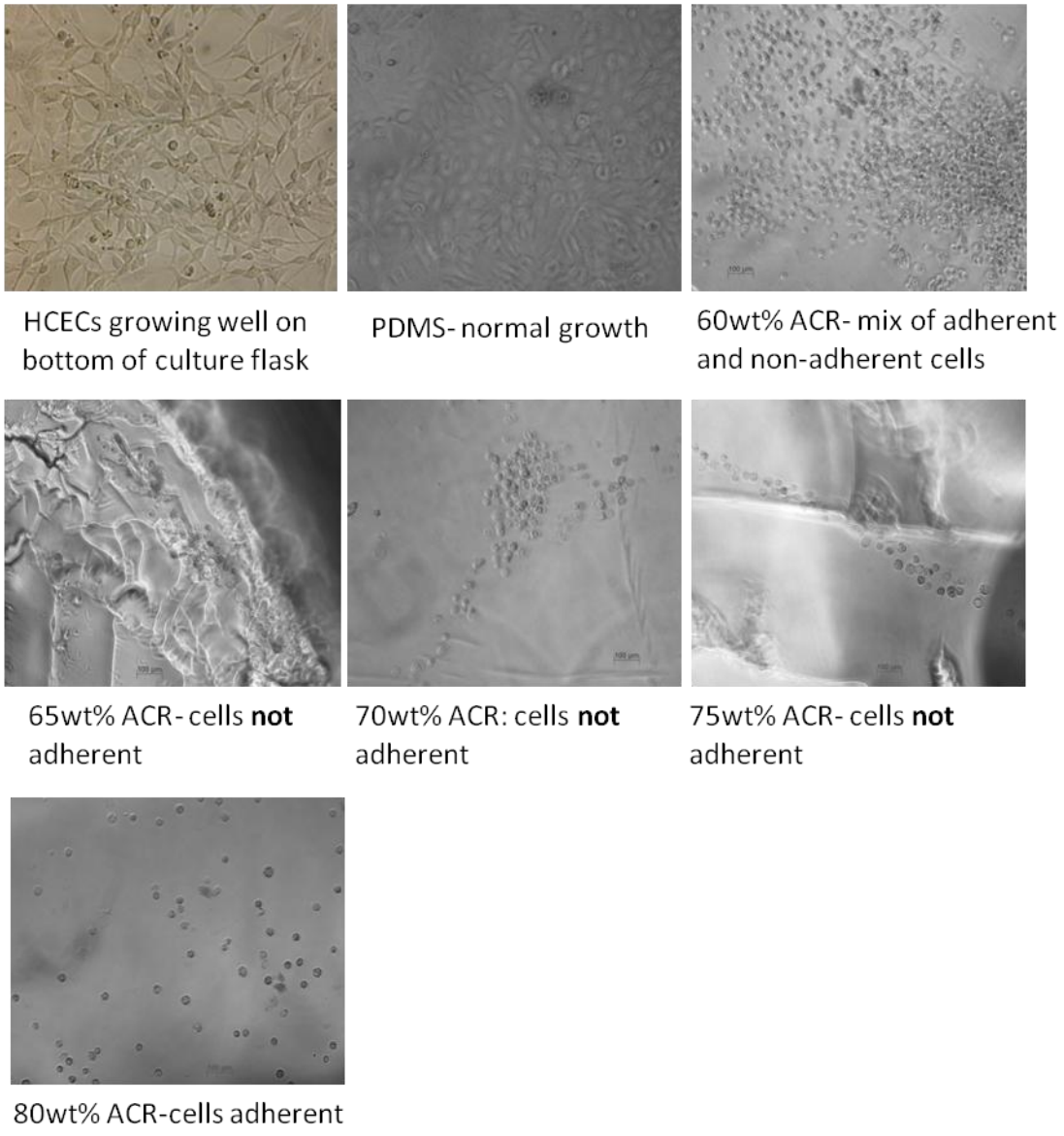

Figure 21: Optical images of 60-80 wt% ACR copolymers seeded with Human Corneal Epithelial Cells (HCECs). Images were obtained using a 10x objective in a Zeiss Axiovert 200 Microscope.

The images depict a HCEC phenotype on the copolymers that vastly differs from that observed on PDMS and the bottom of the culture flask prior to removal via TrypLE^{TM} Express and centrifugation. On the control surface, the cells appeared

elongated and adhered, whereas cells on the copolymers were rounded and in most instances floating in solution. Though the rounded morphology of cells was consistently seen across the copolymer series, adhesion of cells on the surfaces differed with different surfaces. A mix of adherent and non-adherent cells was observed on the 60 wt% ACR copolymer while no cells adhered to any other surface except that of the 80 wt% ACR copolymer.

2.4. Discussion

2.4.1. Factors Affecting Bacterial and Cellular Adhesion

Adhesion of cells is a complex phenomenon that is influenced by numerous factors including, but not limited to, the properties of the materials being adhered to. Commonly cited influences are surface wettability (hydrophilicity/ hydrophobicity), surface roughness and the modulus of the material (stiffness or elasticity).[49] Given the novelty of these polymers, their characterization was necessary to determine their amenability to an adhesion study; ideally, all influential parameters would be consistent across the polymer series with the exception of the variable of interest (surface wettability). The influence of each property on cellular adhesion is discussed prior to analysis of the characterization and adhesion results of the project.

2.4.1.1. Surface Roughness and Topography

Both the roughness and surface topography of materials can significantly affect the adhesion, morphology and orientation of adhering cells and bacteria.[50, 51, 52] Surface roughness (whether accidental or deliberately produced) constitutes a class of

irregularities on an otherwise geometrically ideal (flat) surface.[17] More specifically, a surface is termed rough when the distance between adjacent hills is ~5-100x greater than the depth.[17] Put another way, roughness is a two-dimensional parameter of materials often characterized by an R_a value (the mean deviation of the height profile). [53] Roughness can be periodic or random and can be further classified into macro, micro and nano roughness,[17] each of which can produce different cellular adhesion results.

The influence of surface irregularities on adhesion is clearly emphasized in the report by Tang et al,[53] which examines adhesion of *Staphylococcus epidermidis* to five silicone surfaces of varying roughness prepared by cast molding. The highest and lowest bacterial adhesion was observed on sandpaper and stainless-steel molded surfaces, respectively. Furthermore, cellular adhesion on PEG-based hydrogel materials, which have wettabilities deemed prohibitive to cellular adhesion, can be encouraged through the introduction of roughness using UV-based nano-imprint-lithography.[77] A positive correlation between bacterial adhesion and biomaterial roughness has been reported by several studies.[54,55,56] On exposure to grooved surfaces cells, align themselves in grooves that match the dimensions of the cell size in a process known as 'contact cue guidance'.[57,58,59] An example of this is provided by Jiang et al.[60] who cultured bovine capillary endothelial cells on PDMS samples with well-ordered wave structures (amplitude and wavelength of 2 and 20 μm). They found that the cells adhered and proliferated in the direction of the waves while cells seeded on flat surfaces exhibited random orientation and less elongation.

The different adhesion and proliferation responses are possibly due to substratum topography and demonstrate the importance of indicating not just the presence/ absence of surface roughness or grooves for novel surfaces, but also their characteristics such as size, distribution and periodicity.[61]

2.4.1.2. Substrata hardness

Stiffness and hardness are resistance to elastic (temporary) [62] and plastic (permanent) deformation,[63] respectively, and though separate they are often confused due to their synonymous use in colloquial expressions. Stiffness is measured in Newtons per meter using Young's modulus[62] while hardness can be measured on the Mohs scale (among others) and has three principal operational definitions: scratch hardness,[64] indentation hardness,[64,65] rebound, dynamic/absolute hardness.[63] In the context of literature concerning cellular adhesion , it seems the terms 'hardness', 'stiffness' and 'rigidity' are interchangeable and this synonymy will be continued below.

Although the exact underlying biophysical mechanism is unknown, there is much experimental evidence for the influence of surface rigidities on interfacial adhesion.[66] This is unsurprising since cellular adhesion and proliferation involves complicated molecular signalling pathways[67, 68] based on biomechanical and chemical cues from the underlying extracellular matrix (ECM) in organisms.[69, 70, 71, 72] In fact, researchers at the University of Pennsylvania demonstrated that cultured mesenchymal stem cells (MSCs), which are prototypical of adherent cells for their sensitivity to environmental cues such as substrate hardness, are capable of 'feeling' several microns below the surface to gauge the elasticity of the material, which ultimately determines their fate.[73]

By and large, the literature suggests that cell spreading correlates positively with substrate rigidity so that maximum proliferation is seen when cells are cultured on rigid surfaces like glass coverslips.[74,75,76,77,78,79] A similar phenomenon is reported for bacteria. In one study, the increase in the underlying material stiffness led to increased adhesion of *Staphylococcus epidermidis* and *Escherichia coli* independent of the surface roughness, interaction energy, and charge density of the material.[80] In another study, increasing the concentrations of agar in media (and thereby increasing its rigidity) led to increased production of IV pili required for adhesion on *Pseudomonas aeruginosa* cells.[81]

2.4.1.3. Surface Wettability

The terms 'surface wettability', 'surface free energy' and 'surface tensions' refer to the polar dispersive forces at the surface, which as implied by the definition, are affected by inherent surface chemistry as well as by physical forces.[82] Although high energy surfaces are generally considered hydrophilic, it is the energy differential between the wetting agent and the material that is important, i.e., if the substrate has a higher surface energy than water, then water will wet out the material.[83] Generally, materials with contact angles $< 5°$, $< 90°$, $90° \leq \theta \leq 150°$, $> 150°$ are considered super-hydrophilic, hydrophilic, hydrophobic and super-hydrophobic, respectively.[84,85] It has been shown that the wettability of solid surfaces affects initial adhesion and colonization of bacteria,[86,87,88] as well as cellular adhesion and growth.[89]

Lensen et al. examined the cellular adhesion on extremely high or low wettabilities. Hydrophilic PEG-based hydrogels, tissue culture polystyrene (TCPS), fluoropolymer (poly(vinylidene fluoride), PVDF), perfluorinated polyether (PFPE) and

PDMS were tested. Maximum adhesion by the mouse fibroblast cell line (NIH L929) used occurred on surfaces with intermediate wettability (water contact angle of 55°- 85°). No adhesion or spreading occurred on extremely hydrophilic (PEG-based hydrogels), or extremely hydrophobic (PFPE) surfaces,[49] thereby suggesting the presence of an optimum wettability range for successful adhesion by mouse fibroblast cells.

Bacteria's adhesion response to substrata wettability appears to be strain-dependent,[90] although the hydrophobicity of the material is often implicated in increased bacterial adhesion. For example, *Staphylococcus aureus* adhesion on self-assembled monolayers (SAMs) terminated with methyl (CH_3), carboxylic acid (COOH) and hydroxyl (CH_2OH) groups was found to correlate with the contact angles (100°, 25° and 12° respectively) so that highest adhesion was observed on the methyl terminated surfaces and lowest in this range on the hydroxyl-terminated SAMs.[91] The authors explained this phenomenon with the thermodynamic theory and postulated that hydrophilic surfaces may create stable interfacial water layers, which prevent direct contact between bacteria and the surface and thereby decreasing bacterial adhesion. Hence, as with other material characteristics, the general influence of wettability on adhesion is largely unquestionable.

2.4.1.4. Reason for Differential Adhesion to Material Characteristics

An explanation for the differential adhesion and spreading of cells and bacteria observed in response to different material characteristics (in particular surface roughness and wettability) is that the amount and/or orientation of the initial protein adsorption to these surfaces can vary, which is important since adhered proteins facilitate ensuing cellular adhesion.[92] Nanosize irregularities, for example, are apparently more

advantageous than microscale surface structures for adsorption of cell-adhesion mediating molecules necessary for good subsequent proliferation activity.[93,94,95,96,97] Irregularities < 100 nm are considered analogous to the nanoarchitecture of natural tissues (for example, the size of some ECM molecules) and proteins can be deposited in almost physiological geometrical conformations with exposed bioactive sites for binding to cell adhesion receptors on cells.[98] Surface wettability also affects protein adsorption, and in fact it can also determine whether the adsorbing proteins will undergo structural change or maintain its native conformation.[99] In general, more protein adsorbs to hydrophobic surfaces than hydrophilic surfaces and consequently greater cellular adhesion is often seen on hydrophobic surfaces.[62]

2.4.1.5. The Complexity of Adhesion Studies

Another reason for the discrepancy in adhesion and proliferation results in response to different surface characteristics is the differences between cell lines. Richert et al. [100] immersed titanium disks in various mixtures of H_2SO_4 and H_2O_2 to create nanopits and differing roughness (6nm- 165nm) before examining the adhesion and proliferation of smooth muscle cells (A7r5), fibroblasts (BHK-21) and osteoblasts (UMR-106) on these surfaces. Though cellular attachment in each cell type occurred independently of surface roughness, the subsequent growth of fibroblasts decreased with increasing surface roughness while the contrary effect was seen with osteoblasts. The difference in proliferation was attributed to the activation of different signaling cascades upon biochemical deformation, so that membrane receptor organization and cellular growth was either up- or down-regulated.

In another study comparing the cellular adhesion response to material hardness by fabricating PDMS with different ratios of base to curing agent, Lee et al. reported that the substrate stiffness did not affect the growth of 3T3 fibroblasts and MCT3T3-E1 cells, but HUAEC cells and HELA cells showed cell detachment on stiffer PDMS even before the desired confluency of cells was achieved.[62] In a similar study that varied the curing agent in PDMS samples, Mirzadeh et al. found that mouse L929 cells preferred growth on PDMS with intermediate degrees of crosslinking and stiffness and both higher and lower amounts of curing agent induced less cell adhesion and spreading.[101]

Like mammalian cells, different bacterial strains also respond differently to micro-environmental cues. Truong et al., for example, showed that *Staphylococcus aureus* CIP 65.8 had a significantly greater ($t = 0.002$, $p < 0.05$) propensity for attachment than *Pseudomonas aeruginosa* ATCC 9025 to surfaces of commercial purity titanium (CP, Grade-2) that had nanoirregularities introduced to them via equal channel angular pressing (ECAP), than those without.[102] They attributed the differential adhesion and subsequent biofilm formation to the morphological differences between the two strains; the patterned nanostructures on the ECAP-processed surfaces were said to be more amenable to anchoring by the spherical *S. aureus* cells than the rod-shaped *P. aeruginosa* bacteria. Hence, the cellular or bacterial response of one type of line or strain cannot be extrapolated to others.

The generalization of adhesion results is further complicated by the interrelation of material characteristics. Surface roughness, for example, affects the surface wettability so that the spreading and receding of water on materials with initial contact angles

between 45° and 90°can be controlled with varying the roughness (i.e., the height, width and distribution of surface irregularities). [103] Shibuichi et al.[104] for example found that increasing the surface roughness of a material increased its hydrophobicity, a fact supported by Veeramasuneni et al.[105] who reported that increases in roughness at the nanoscale increased the contact angles of hydrophobic PTFE (poly-tetrafluoroethylene) due to the drop edge being 'arrested' by the borders of grooves.[106,103] This relation between material characteristics along with the differences between cells and strains points to the importance of contextualizing all adhesion studies for the application, material and cell types used to prevent erroneous generalization and oversimplification of the problem of undesirable cellular/bacterial adhesion.

2.4.2. Analysis of Characterization, Biocompatibility and Adhesion Results

2.4.2.1. Need for Reaction and Polymer Extraction Optimization

Unintentional flaws introduced to the copolymer surfaces during polymerization or coupon extraction can adversely affect the validity of adhesion responses. Hence understanding potential causes of observed artifacts can help mitigate such bias and ensure meaningful results. Though the increasing weight percent of ACR in the copolymers prepared in this study qualitatively increased the softness of the materials and thereby facilitated subsequent removal of coupons from the disk, it also correlated with increased 'buckling' of the polymer surface [Figure 22.b] and an increased amount of unreacted starting material on the polymers after polymerization [Figure 22.a]. Both observations may result from free radicals being quenched by oxygen[107,108] in the layer of monomers that phase separated to the surface. This is likely given the high permeability

of siloxanes to oxygen and the presence of siloxanes in ACR. In such a model, the underlying layers of monomers, which may not contain a homogenous dispersion of reagents, will have different cross-linking densities due to a diffusion induced concentration gradient of oxygen. This inhibits polymerization and produces in-plane stresses that cause surface wrinkling. [108] The use of a nitrogen atmosphere during polymer synthesis and a better photoinitiating system are two ways in which the macro roughness of copolymers thus produced can be controlled to limit influence on adhesion data. In the interim, running NMRs on the liquid films will help identify their composition, though ACR may comprise the bulk of these residual layers given their quantity appeared to increase with increasing weight percent ACR. Preferential loss of ACR from the system, which may be occurring on account of faster cure rates of HEMA, was not limited to the polymerization step; the percent weight loss of the copolymers after extraction in propanol increased with increasing weight percent ACR [Figure 16], while NMR analysis over the 12 hour extraction period identified the predominant leachant as the surfactant [Table]. The latter result also explains why larger zones of inhibition were seen around copolymers of higher ACR weight percentages [Figure 14]; ACR was leaching to a greater degree than HEMA. In order to determine the optimal extraction time, spectra of the aliquots taken at time-points past 30 minutes need to be analyzed. The optimal time s will correspond to a plateau in integration values for the leachants.

a) 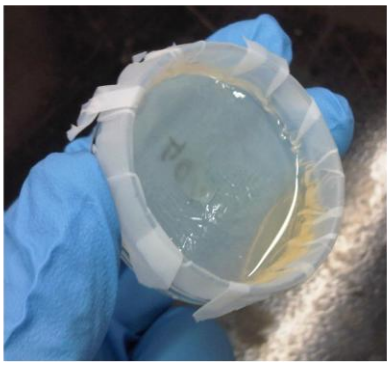 b) 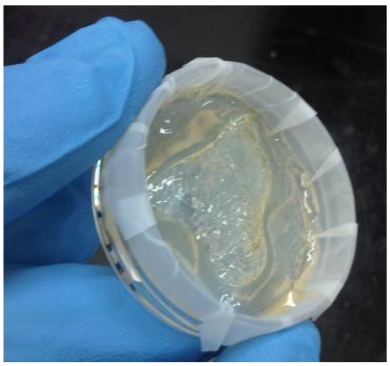

Figure 22: Appearance of two representative copolymers after synthesis: a) 60 wt% ACR copolymer with a thin film of unreacted starting material after 30 min of irradiation with UV light, and b) 80 wt% ACR copolymer with surface wrinkling.

This loss of ACR was problematic on two counts: 1) it likely contributed to the unchanging contact angles across the polymer series by facilitating the provision of a consistent interface; and, 2) the bulk loss of starting material from the middle of the copolymer disks produced coupons with slanted surfaces that produced variability in the measurements of material characteristics. Large variation was also observed between replicate measurements of samples in the biological studies, but this was due to artifacts produced during coupon extraction from polymer disks. Copolymers with higher weight percentages of HEMA for example had a tendency to crack and shatter when 'punched' so that at times the coupons obtained were not all of the same diameter. For all these reasons, perfecting the acquisition of materials for future adhesion assays appears paramount.

2.4.2.1. High Optical Transparency of ACR-HEMA copolymers

Although the degree of light transmittance through potential biomaterials is not a property that affects cellular adhesion, it is a desirable property for certain applications, particularly in the ophthalmic industry, hence it was deemed necessary to quantify. All copolymers with the exception of 60 wt% ACR, which was cloudy with a yellowish tint, were highly transparent over the range of visible light wavelengths (400-750nm).[109] The reason for this discolouration is not evident, while its observation in multiple batches of synthesized copolymers, even from fresh stocks of reagents, seems to eliminate the possibility of contaminants. Other differences between copolymers are a direct consequence of artifacts produced during coupon extraction and the varying thicknesses of coupons (~1-2 mm) even from the same copolymer disk due to loss of ACR after 12 hours of swelling in isopropanol. Punching coupons from the rigid poly-HEMA disk for example, created surface cracks that are known to hinder light transmission[110] hence its transmittance of ~52%. Similarly, the friable nature of poly-ACR coupled with the tendency of its surface to spontaneously buckle created surface irregularities that impaired light transmittance despite the polymer appearing highly transparent when observed qualitatively. Varying thickness of coupons was a concern, not only because it comprised consistency within the experiment, but also because its affects the path length of light through the material and consequently the overall transmittance.[110] The interesting increase of transmittance over ~400- 450 nm for all copolymers may simply be a function of how the shorter wavelengths in this region interact with the material and its surface artifacts (as is the case with Rayleigh scattering),[111] or, since the gradient of the slope

during this increase varies between copolymer formulations, the increase may be a result of the chemistry. It is important to note that the light transmittance of these copolymers for its intrinsic interest, and not specifically to justify the use of these copolymers as ophthalmic biomaterials such as lenses. Had the latter been the case, then light transmittance for a hydrated set of coupons in saline would also have been measured, along with the refractive indices of each formulation as suggested by the FDA.[112] Though values for the minimum light transmittance of lens materials could not be found, conversations with others in this area of research suggest that > 80% light transmittance for potential biomaterials is a good start when considering ophthalmic applications, and that lens materials typically require an anti-reflective coating to increase their transmittance past 92%.[113]

2.4.2.1. Increasing Water Uptake with Increasing ACR Content

Given the water uptake of ACR-HEMA copolymers as is evident from Figure 9, the materials may be termed hydrogels (polymer networks capable of imbibing large amounts of water while retaining their three-dimensional structure),[114] in which case their swelling may be similarly described. When dehydrated, the close proximity of polymer chains in hydrogels limits inward diffusion of molecules.[115] Upon immersion in water, however, the osmotic differential between spaces within the matrix and the external environment induces water penetration of the polymer network,[115] and as the material swells, the chains separate to the extent permissible by the elastic retractile force of the network, which is determined by crosslinkers in the system.[115,116] Since water uptake for the copolymers increases between 60 and 75 wt% ACR, and is slightly higher

during this range than the water uptake for poly-HEMA, ACR is clearly enhancing the hydrogel-like behavior of these materials. This phenomenon may be attributed to both the hydrophilic nature of the surfactant's long PEO chains and the relatively larger initial 'space' they may create in the final dry product when compared with the shorter HEMA monomers. The presence of ACR in the matrix may also allow for greater expansion upon water uptake, since crosslinking of the ACR molecule would occur mainly at its acrylate-end leaving the large PEO chains physically entangled but free to separate in response to an appropriate pressure. However, ACR's additive effect on water absorption appears limited within a certain range seeing as poly-ACR, 60 and 80 wt% ACR copolymers have very similar percent water uptakes.

As expected, poly-ACR absorbs less water than poly-HEMA (~12% less) due to the presence of its hydrophobic head groups that would limit inward osmosis. Since PDMS is generally regarded as a hydrophobic material, its 8% water uptake seems strangely high, but may be attributed to contamination during synthesis; all 6 coupons were extracted from one PDMS elastomer hence each would be affected by introduced impurities.

Other interesting observations during the water uptake study include the increased tackiness of hydrated copolymer coupons vs. dry ones and the formation of air bubbles on the interfaces of copolymers immersed in water [Figure 11]. The term 'tack' refers to the sticky feel of a material, which is not necessarily related to the adhesive strength of the same.[117] It is largely associated with the material's viscoelasticity, since this property allows enough material 'flow' for conformal surface contact to facilitate hydrophobic or

van der Waals interactions, while ensuring the material retains enough cohesive strength to resist bulk failure.[118,119,120121,122] Explanation of a material's tack therefore requires some quantification of rheological properties, but since this data has not been collected and was not the focus of this project, a satisfactory reason may not be given at this time. It can, however, be assumed that hydration of these elastomeric copolymers alters the surface chemistry (via rearrangement of surface groups) in a way that facilitates tack, and that the decrease in adhesion observed after repeated stick and peels of the coupons from the weighing boat is a result of the surface changes that occur during detachment of the copolymer, such as particulate contamination.[123] The reason for the formation of bubbles is also not well-understood.

2.4.2.1. Consistent Hardness and Wettability across Copolymer Series

As aforementioned, hardness is defined as a material's resistance to indentation by a static load, so the larger the resistance to deformation, the harder the material.[124] Since the plastic deformation of the material is involved in hardness measurements, the hardness test should be repeated only at different sites on the material surface to avoid invalid results.[124] Furthermore, the testing device must be clearly defined given the multitude of measuring instruments available for hardness and the fact that it is not considered a fundamental physical property[124] For laboratory setting measurements of hardness, the Shore Durometer device is most commonly employed on account of its simplicity and portability. It is recognized that the hand-held nature of the device and its use of springs to generate the indenting pressure makes the measurements neither highly precise nor reproducible, however, the technique is still viable and more complicated

analyses need only be performed when the material has well-defined application parameters.[125] This is not the case for the ACR-HEMA copolymers, so the Shore 00 durometer (the type of durometer used for soft materials and foams), was utilized. Surface wettability is typically measured using one of several contact angle measurement techniques, but the sessile drop (liquid on a solid surface) and captive bubble (a fluid bubble introduced to a solid surface immersed in a liquid) are two favored types.[126] The latter was used first for the ACR-HEMA copolymers given their tendency to swell in water; it was thought that absorption of the droplet using the sessile technique may be problematic and result in false identification of the materials as hydrophilic. However, the variance seen within measurements for each copolymer type and the consequently large error bars necessitated the use the sessile-drop technique, which was deemed more robust since its set-up involved fewer steps (and therefore had less room for error) and the measurements were obtained from digital photographs. Given that there was little difference in contact angles obtained using the sessile drop goniometer at 0 and 3 minutes [Figure 12] for dry copolymers (with the exception of poly-ACR), it seems that the concern regarding droplet absorption was unnecessary. This may be because water absorption occurs as a function of time; perhaps a greater difference from sessile drop contact angles at 0 minutes may have been observed had measurements been obtained after a longer time interval. This may be the case seeing as the percent water uptake for all copolymers was calculated after their complete immersion in water for 30 minutes. Regardless, it is the consistency in contact angles obtained via either method that has greater import in the context of adhesion, since the project concerns analysis of the later

in response to variance of the first. Since EDX analysis suggests equal dispersion of silicon in the system and therefore possible surface saturation with ACR for each copolymer type, the consistency in surface wettability is understandable.

2.4.2.2. Antibacterial Activity of ACR Monomers

Given the surfactant nature of ACR and the fact that surfactants are important constituents of disinfectants,[127] the potential antimicrobial activity of these polymer coupons was deemed interesting to discern prior to adhesion studies. An adaption of the Kirby-Bauer test was utilized for this purpose. The assay, also known as the disk-diffusion method is a simple, rapid and standardized *in vitro* technique used to ascertain antimicrobial activity, and is approved by the Food and Drug Administration (FDA).[128,129,130] Modified versions of the test have also been used for testing the antibacterial properties of polymers, where clear areas of interrupted bacterial growth directly under the material serve as an indication of antibacterial properties.[131] The test typically involves growth of a known concentration of a bacteria strain on Mueller-Hinton agar, and the measurement and comparison of the zones of inhibition (areas devoid of bacterial growth) produced around circular disks of filter paper, which are placed on the cultured lawn and impregnated with known concentrations of antibiotics.[132] However, for a quick qualitative comparison Luria-Bertani (LB) agar was selected since it is both a rich generic media suitable for growing strains like *Escherichia coli* (*E. coli*) and is widely available.[133]

Though the Kirby-Bauer technique did not indicate antibacterial activity of the copolymers (no zones of inhibition were seen around or under extracted coupons), it

clearly indicated: 1) the problem of leachants and the necessity of extraction prior to biological experiments; and 2) the toxicity of both ACR and HEMA to *E. coli* in their monomeric forms. The cytotoxicity of ACR was expected, since surfactants are known to dissolve the phospholipid bilayers of bacterial cell membranes, which can no longer regulate the movement of molecules into and out of the cell as a consequence. Many mechanistic pathways for surfactant-induced solubilization of membranes have been described to accommodate different types of surfactants and membranes,[134,135,136,137,138] but generally the process has been reported to occur in three steps.[139,140,141,142,143,144,145,146] The first step involves integration of the surfactant into the bilayer, which continues until a critical value is exceeded and mixed micelles containing both some surfactant and membrane components disassociate from the rest of the layer. This detachment and coexistence of surfactant-saturated membranes with micelles in solution constitutes stage two. Though the cell membrane would still be intact at this point, its integrity has been compromised, and cell lysis is typical by the third stage when complete dissolution of the membrane into mixed micelles occurs. In the case of ACR, the trisiloxane head group may be integrating with the hydrophobic core of the bilayer, resulting in eventual bond disruption between adjacent phospholipids. The mechanism by which HEMA is cytotoxic is not as clear, and despite its reported ability to induce apoptotic cell death in HeLa S3 cells,[147] peripheral blood mononuclear cells[148] and human[149] and mouse fibroblasts,[150] there appear to be no studies on the anti*bacterial* activity of HEMA. It is postulated that as with surfactants, methacrylate monomers can both integrate into membrane bilayers to cause solubilization of the lipids found therein,[151] and that the presence of a hydroxyl

group in methacrylates enhances their cytotoxicity.[147] Another study also attributes import to the hydroxyl group and suggests that its dehydration in proximity to biomembranes confers hydrophobicity to the molecule and thereby facilitates its integration into the bilayer.[152] However, if the presence of a hydroxyl group on a hydrophilic molecule was all that was required for disruption of bonds between phospholipids in membranes, then almost any hydrophilic molecule could penetrate bilayers and this is not the case. Hence the exact mode of action for HEMA's cytotoxicity still requires elucidation.

2.4.2.1. *E. coli* Adhesion on Copolymers

Despite the relatively good (albeit consistent) data obtained from the adhesion assay in its first run [Figure 17], the unfortunate lack of values for poly-HEMA and PDMS necessitated a repeat of the assay for dry coupons, while a suggestion that water uptake may correlate positively with bacterial adhesion at an NSERC 20-20 Ophthalmic Network Meeting prompted the additional use of hydrated coupons in the assay. However, the new data [Figure 18] appears to be so nonsensical that its utility is easily questionable. For one thing, the minimal fluorescence seen for PDMS (141 RFUs, contact angle 100.1°, Figure 12)in comparison to poly-HEMA (211 RFUs, contact angle 54.7°, Figure 12) seems contrary to the literature, which routinely quotes hydrophobic surfaces as facilitating bacterial adhesion (particularly that of *E. coli*, a gram-negative[153] strain) to a greater degree than hydrophilic ones.[91,154] Other concerns include the: 1) lack of consistency, which was predicted by the consistent material characteristics; 2) the fact that negative fluorescence is seen at random for both hydrated and non-hydrated coupons; and, last but not least, 3) the large errors bars. These concerns and their potential causes

will be discussed in more detail later. The inclusion of this data then serves the dual purpose of emphasizing the clear difference between adhesion to poly-ACR and the copolymers in both cases, and of illuminating the significance of quenching effects in fluorescence-based assays.

At first, and based on the suggestion received at the network meeting, it was thought that poly-ACR's ability to imbibe water caused the observation of increased adhesion. However, since all copolymers including poly-HEMA showed greater water uptake than poly-ACR [Figure 9], this variable, though perhaps influential, is likely not the sole determinant of our observation. Poly-ACR's pliability, in comparison to other copolymers and in accordance with the Shore hardness data, may be consequential [Figure 8], but the difference between its hardness and that of the next lowest is a mere 6.83 durometer points that is made even less significant by the overlap of the error bars for these two points. Similarly there is little difference between sessile drop contact angles and surface roughness of dry poly-ACR and copolymer coupons. As it turns out, the reason for increased adhesion may be due to greater surface roughness at the macro scale for poly-ACR than other coupons as shown in Figure 23.

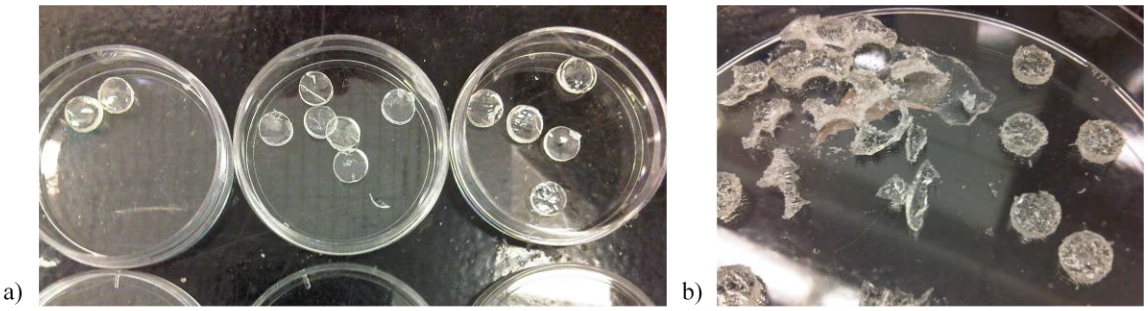

Figure 23: Macroscale surface topography of a) poly-HEMA, 65 wt% and 80 wt% ACR copolymer coupons (from left to right), and b) poly-ACR coupons. While all other surfaces are flat and comparable, the surfaces of poly-ACR are not.

Whereas the large errors bars seen in data set 2 are a consequence of imperfect polymers as discussed in section 2.4.2.1, the negative fluorescence and lack of consistency as compared to the first set of results is possibly due to quenching and autofluorescence.[155] Qualitative adhesion studies using green fluorescent protein (GFP) were conducted due to the accessibility of both IPTG and a GFP-producing *E. coli* strain, as well as the advantageous nature of GFP as a fluorophore; its expression eliminates the need for fixation of the organism or the addition of potentially deleterious chemical substrates or cofactors for visualization, while the mechanism for its fluorescence appears self-contained and does not pose a metabolic burden on its host.[156] However, biological fluorophores such as GFP do not typically exhibit the same photostability as that of synthetic fluorescent dyes[157] and are therefore susceptible to quenching by other molecules in solution such as oxygen[158], and their fluorescence can be obscured by high background fluorescence caused by sample autofluorescence when using shorter wavelengths of light (< 500 nm).[157] In the case of data set 2, the fluorescence of the samples could not be measured immediately due to equipment inaccessibility, and the

samples were left in darkness for 8 hours overnight. The quenching that may have occurred coupled with the autofluorescence of the samples (since the excitation wavelength of GFP is 395 nm (< 500 nm)) most likely resulted in the negative fluorescence values observed. Hence for the interpretation of adhesion results, the data presented in figure 1, imperfect as it may be without its controls, has been utilized.

Ordinarily, and particularly in light of the discussion for factors affecting cellular adhesion, I would try to determine the optimal surface roughness, surface wettabiltity and surface stiffness specific for the adhesion and proliferation of *E. coli* and interpret the results of this study within that context. However, since there is absolutely no variation in either surface properties or bacterial adhesion and given the quagmire of contention and incompleteness in the literature, there may be little sense in such an attempt. Even if such information was readily accessible, its applicability would be limited given the novelty of these copolymers. Consequently, the only conclusions that can be drawn from this study are that *E. coli* is adhering to these polymers and that the adhesion is consistent across the series, both of which are justifiable since *E. coli* is a relatively hydrophobic strain that is said to preferentially bind to relatively hydrophobic materials[153], and since there is no significant difference between the surface characteristics of the different copolymer types.

In order to explain this phenomenon, the relative fluorescence units (RFUs) obtained from the adhesion studies on the copolymers were plotted against the sessile-drop contact angles [Figure 19] and the percent water uptake for the set [Figure 20]. The two graphs exhibited a slight positive and negative correlation respectively, but the low

R^2 value of each (0.423 and 0.1138) prevents the use of either variable as a predictor for *E. coli* adhesion to this set.

2.4.2.2. Potential Incompatibility of Copolymers and HCECs

Human corneal epithelial cells were selected for biocompatibility testing with mammalian cells given their robust nature, accessibility and ability to propagate in serum-free media. The rounded morphology of cells observed on all copolymer types is atypical, whereas the elongated morphology of HCECs observed on PDMS and in the culture flask is characteristic of adhesion and subsequent proliferation[159] [Figure 21]. The aberrant morphology coupled with the observation of HCECs free-floating in solution instead of settling on the copolymer surfaces (with the exception of 60 wt% ACR) suggests that the cells were dead. If the cells had been alive but considered the surface undesirable for attachment, then adhesion and proliferation may have been observed below the coupon on the bottom of the culture flask, but this was not the case. Still, a live-dead stain such as that based on calcein and ethidium homodimers is needed to validate a claim of cytotoxicity. If the materials are indeed cytotoxic, then it would be interesting to determine the source of the toxicity, but given the absence of poly-ACR and poly-HEMA in the assay, neither HEMA, nor ACR, nor the combination of the two can be assigned blame and consequently a mechanism for cytoxicity cannot be hypothesized. Similarly, the reason for some adherence of HCECs on 60 wt% ACR surfaces and not others cannot be elucidated at present.

2.5. Conclusions

Novel, optically clear copolymers of ACR-HEMA were created that exhibited consistent surface hardness, roughness, wettability and therefore relative *E. coli* adhesion, despite the systematic variance of ACR and HEMA in the matrix and contrary to our hypothesized effect of the latter. As such it is impossible to determine the effect of varying surface wettability on bacterial adhesion based on these materials in their current state. Furthermore, qualitative biocompatibility testing with HCECs suggested potential toxicity to mammalian cells since a round, non-adherent morphology was consistently seen across the copolymer surfaces. The consistency of contact angles likely results from a consistent interface despite changes in bulk composition due to inadequate participation of the surfactant in the polymerization process; ACR was the main leachate during copolymer extraction in propanol for 12 hours. Optimizing the polymerization process via use of better photoinitiators, for example, may ensure ACR participation and will reduce the large standard deviations seen for replicate measurements. In the interim, a novel set of ACR-based polymers were created in which the HEMA had been substituted with hydrophobic monomers with the hope of achieving varied surface wettability.

3. Chapter 3: *E. coli* Adhesion on Polymers of ACR, BMA and MMA

3.1. Introduction

Butyl Methacrylate (BMA) and Methyl Methacrylate (MMA) [Figure 24] are compounds of the methacrylate family used in the plastic manufacturing, printing, cosmetic and biomedical industries.[160] Their uses in the latter comprise of medical implants, dental prostheses and surgical bone cements among other things.[160,161] Although methyl methacrylate is the more commercially important monomer, both have desirable properties in their polymeric form, such as optical transparency, general biocompatibility,[161] strength, general moisture resistance and particularly hardness.[160]

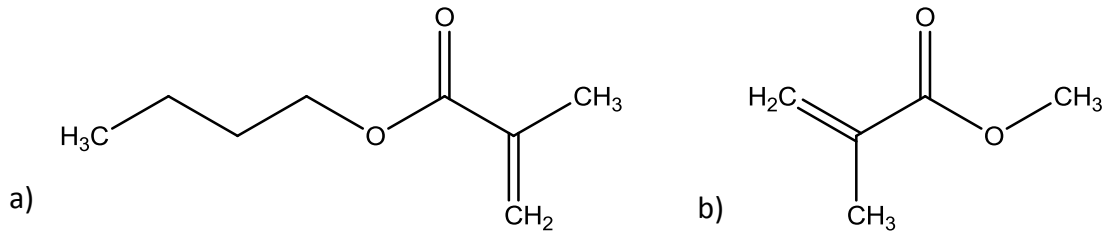

Figure 24: Chemical structures of a) Butyl Methacrylate (BMA) and b) Methyl Methacrylate (MMA) monomers.

Their contribution of hardness and mechanical strength to polymer blends has made the two useful additives to silicone materials, which have their own unique properties [detailed in section 1.3]. Silicone-methacrylate hybrids have been used in lens materials and pressure sensitive adhesives among other things due to their relatively excellent antifouling and corrosion resistance, their ability for facile incorporation into aqueous emulsions and their high tolerance to a range of chemicals and temperatures.[162] In the context of project 2 for this thesis, it was hypothesized that controlled surface

wettability of materials could be induced by replacing hydroxyethyl methacrylate (a known hydrophillic monomer)[43] with butyl or methyl methacrylate (hydrophobic monomers)[163,164] when polymerizing with ACR, since this would make the remainder of the polymer sufficiently different from the ACR that also contains a large hydrophilic chain (poly (ethylene oxide) (PEO)). Furthermore, these strongly hydrophobic components of the new materials could theoretically decrease their water uptake, a property which may affect bacterial adhesion though no such correlation was evident for the HEMA-ACR copolymers.

Polymerization of methacrylate monomers typically involves irradiation with ultraviolet (UV) light, a process that can be accelerated with the addition of photoinitiators,[160] since the latter produce the reactive species necessary to commence radical chain polymerization.[165] The photoinitiating system of choice for hard materials comprised of methacrylates is that of camphorquinone (CQ) and 4-dimethylamino benzoate, which are excited by visible blue light (420–500 nm).[166] Hence these reagents were acquired and utilized in a synthesis protocol similar to that of the ACR-HEMA copolymers, with the ultimate goal of varying surface wettability and examining bacterial adhesion as a result for comparison to the materials used in Chapter 2.

3.2. Materials and Methods

3.2.1. Materials

Camphorquinone (CQ), hydroquinone monomethyl ether (MEHQ) inhibitor remover, 4-dimethylamino benzoate (AH), methyl methacrylate (MMA), butyl

methacrylate (BMA) and diethylene glycol diacrylate (DEGDA) were purchased from Sigma Aldrich. The silmer ACR A008-UP (ACR) was a gift from the Siltech Corporation and stored at -20 °C. Inhibitors were removed from the BMA and MMA were via passage through a MEHQ-packed column and stored in amber bottles along with the DEGDA at 2 °C. All polymers were synthesized to have a final weight of ~2 g, 1 wt% CQ and 1 wt% AH as radical co-photoiniators, 1 wt% DEGDA as the crosslinker and varying weight percentages of ACR at 10 wt% intervals (from 0 to 100 wt%) while the remaining weight of the polymer was divided equally between BMA and MMA. The general synthesis is exemplified with the procedure for the copolymer containing 60 wt% ACR, 20 wt% MMA and 20 wt% BMA

3.2.2. Methods

3.2.2.1. Polymer Synthesis[1]

CQ (0.02 g, 1 wt %), AH (0.02 g, 1 wt %), inhibitor-free MMA (0.04 g, 20 wt %), BMA (0.04 g, 20 wt %) and DEGDA (0.02 g, 1 wt %) were weighed into a 10 mL glass test tube in that order. The mixture was stirred until homogenous and ACR (1.2 g, 60 wt %) was added. The resulting solution was deoxygenated by purging the system with N_2 (g) for 30 s and transferred into a Teflon-lined petri-dish before irradiation for 30 min under a blue light source provided by Kerber Science (480 nm). The solid elastomer thus formed was extracted in 40 mL of 2-propanol for 12 h then dried in a vacuum oven (50

[1] Protocol created by Nicholas Luong as part of his MSc thesis.

°C, 51 mm Hg). A 0.635 mm punching tool was used to obtain circular disks for subsequent experiments.

3.2.2.2. Sessile-Drop Contact Angles and Water Uptake

The contact angle data was graciously provided by a colleague in the Brook lab, Nicholas Luong. Briefly, a Ramé-Hart NRL C.A. goniometer and 0.02 mL of Milli-Q per coupon surface was used to obtain contact angles for dry polymer disks (n = 3 for each type). The drop profiles on coupons were photographed after 3 min using the Krüss Drop Shape Analysis software (v.10) and GIMP2 Image Analysis Software was subsequently used to measure and average the contact angles on either side of the drop in each image. Average static sessile- drop contact angles were plotted for comparison between polymers. The average percent water uptake for 6 coupons of each polymer from the ACR-MMA-BMA polymer series was obtained by measuring the weight of coupons before and after immersion in dH_2O for 30 min.

3.2.2.3. *Escherichia coli* Adhesion Study

A pre-synthesized, sterile LB agar plate (~12 mL of a mixture containing 10 g of tryptone, 5 g of yeast extract, 10 g of NaCl, 15 g of agar and 1 L of distilled water) and 100 µL of pre-made working solution of *E. coli* as described earlier [Section 2.2.4] were incubated in preparation for the adhesion assay. Since the protocol for the assay has been detailed in full in section 2.2.6, only a short summary has been provided here. Multiple colonies (3-4) from the plate were aseptically transferred into 200 mL of broth, which was subsequently incubated. *E. coli* growth in the solution was monitored via

measurement of the OD_{600} of 1 mL aliquots obtained every 30 min. Once the OD_{600} had reached 0.7, 0.5-1 mM, IPTG was added to the vial before an additional 5-6 h of incubation. The *E. coli* was subsequently filtered into 100 mL of PBS that was supplemented with 2% w/v nutrient broth. Four coupons from each polymer type were incubated with 400 µL each of the solution for 12 h, after which they were rinsed thrice with autoclaved PBS and placed in a fresh 48- well polystyrene, flat-bottom plate. A Gemini XPS microplate reader was used to obtain GFP fluorescence readings (excitation and emission wavelengths of 395 nm and 509 nm respectively). The average fluorescence readings were plotted for comparison, and then plotted against the contact angles for each polymer to determine the correlation (if any) between surface wettability and *E. coli* adhesion.

3.3. Results

3.3.1. Varying Contact Angles and Increasing Water Uptake across Series

The Krüss Drop Shape Analysis software (v.10), loaded on a Rame´ Hart NRL C.A. goniometer (Mountain Lakes, NJ), was used to photograph the sessile- drop profiles of Milli-Q water introduced to 6 disks of each polymer type. GIMP2 Image Analysis Software was used to measure the average angle for each image, and the average contact angle data for each polymer was plotted against the weight percent ACR in Figure 25.

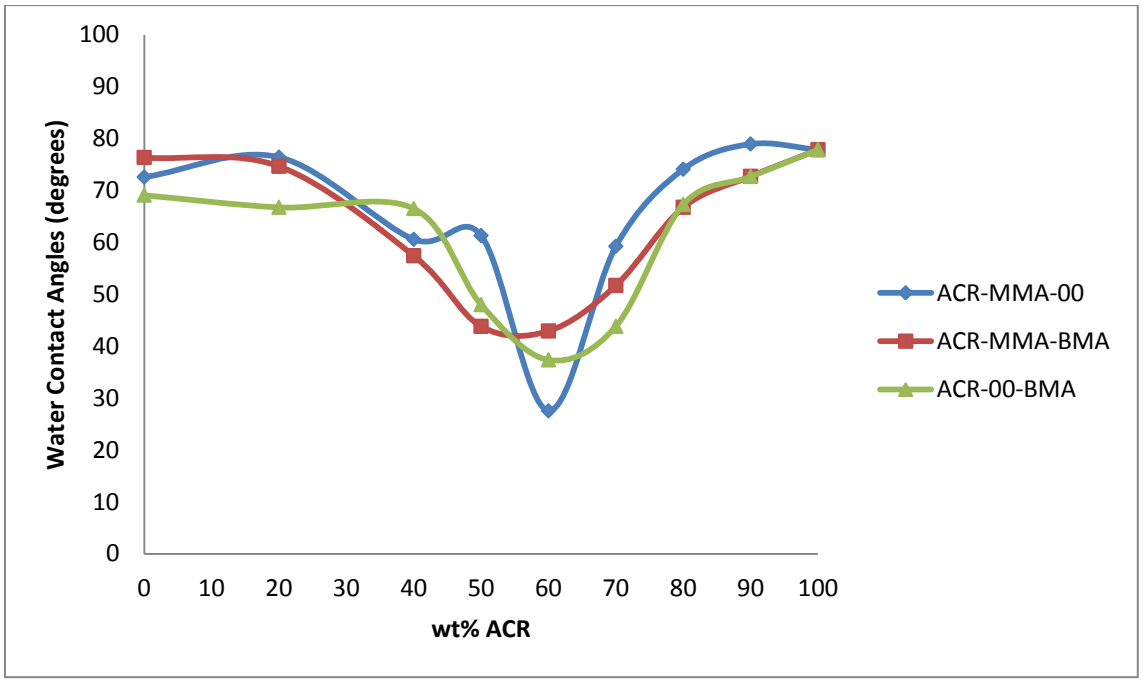

Figure 25: Contact angles obtained for the different ACR-MMA-BMA polymers.

Polymers with lower and higher weight percent ACR (≤20 wt% and ≥80 wt%) appeared to be moderately hydrophillic with contact angles in the range of ~67°- 77°. Between 20 and 80 wt% ACR polymers however, the contact angles dipped (suggesting increasing surface wettability) to a low of 27.6°- 42.9° for the ACR-MMA and ACR-MMA-BMA series respectively.

The water uptake study, however, yielded a relatively straightforward positive correlation between increasing weight percent ACR and the percent water uptake for the ACR-MMA-BMA series [Figure 26]. The highest uptake (18.2%) was seen for poly-ACR while no uptake was observed for the MMA-BMA polymer coupons. Poly-BMA and Poly-MMA values had the second and third lowest uptake values (0.5% and 2.4%) respectively. A much larger uptake difference was observed between the 80 wt% ACR

and 100 wt% ACR than between other wt% ACR polymers (11.9% vs. 2.6% between 60 wt% ACR and 80 wt% ACR).

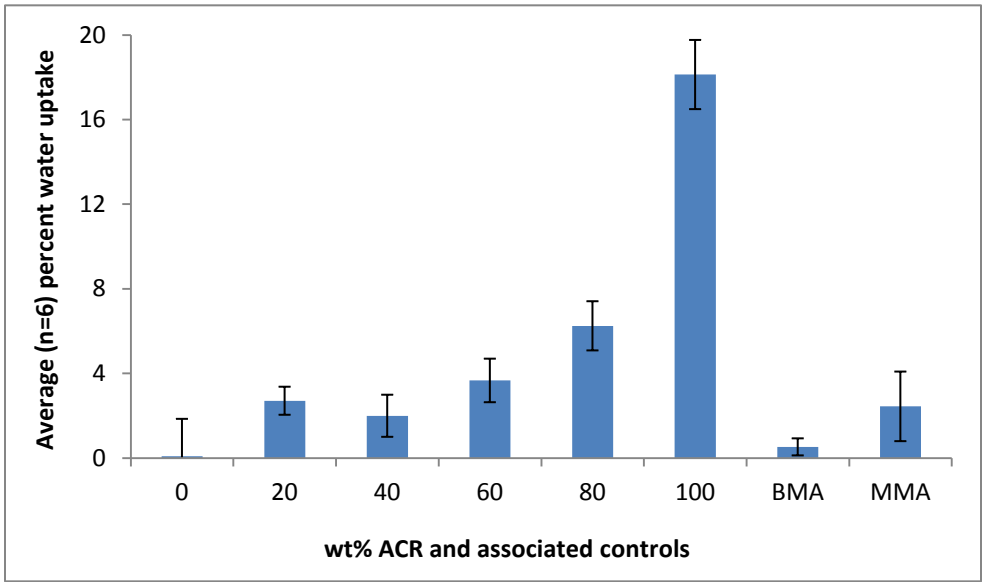

Figure 26: Percent water uptake of the polymers in the ACR-MMA-BMA series.

3.3.1. Increasing *E. coli* Adhesion with Increasing Weight Percent ACR

Bacterial adhesion measurements were conducted in a similar manner to those specified for the ACR-HEMA copolymers. Coupons (n = 4) for each leachate-free polymer in the three series were incubated for 12 hours at 37 °C with 400 µL each of PBS inoculated with IPTG-induced *E. coli* and supplemented with 2% w/v nutrient broth. The coupons were then rinsed thrice with PBS, placed in a 48-well plate, and GFP fluorescence from the surfaces was measured using a microplate reader (Gemini XPS). The readings, taken at an excitation and emission wavelength of 395 and 509 nm respectively, were plotted both individually [Figure 27] and against contact angles

[**Figure 28**] for the purposes of comparison.

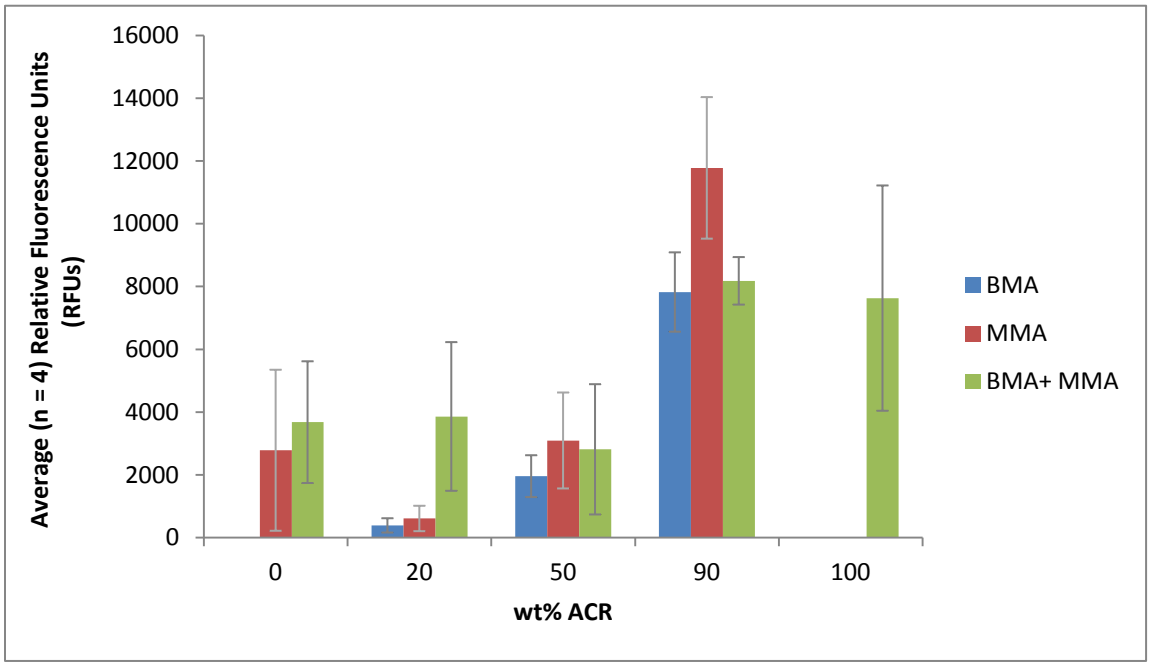

Figure 27: Average (n = 4) relative GFP fluorescence readings from IPTG-induced *Escherichia coli* adhered to polymer surfaces for the ACR-BMA, ACR-MMA and ACR-MMA-BMA series.

Higher RFUs were seen for higher weight percentages of ACR in each polymer series. The greatest value was observed for 90 wt% ACR in the ACR-MMA material (11,777.75 RFUs), which, based on the error bars, was significantly higher than those following it (8179.5 and 7823 RFUs for 90 wt% ACR polymers of the ACR-BMA and ACR-BMA-MMA series accordingly). The 20 wt% ACR polymers for the ACR-BMA and ACR-MMA group showed the lowest RFUs (388.75 and 3,859 RFUs), which were also significantly different from the ACR-BMA-MMA polymer of the same ACR weight

percent. For the rest of the ACR weight percentages, fluorescence readings appeared to be no different among the three series on account of the overlapping errors bars.

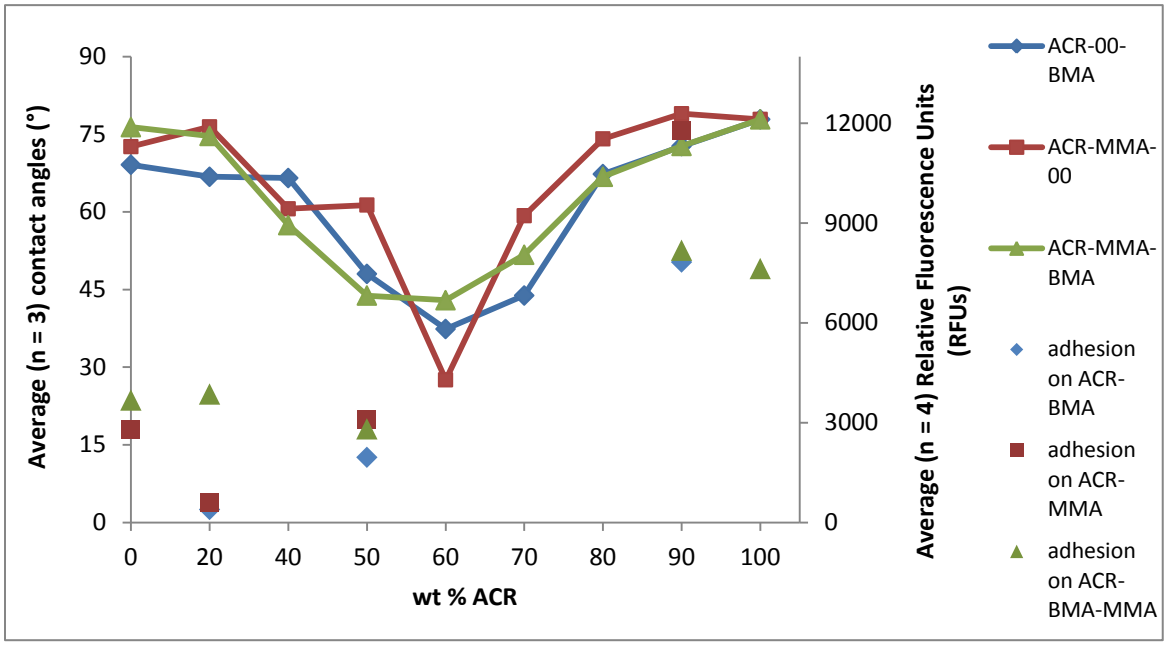

Figure 28: Average (n = 4) GFP fluorescence readings vs. the average (n = 3) sessile-drop contact angles for the ACR-MMA, ACR-BMA and ACR-MMA-BMA polymer series.

According to Figure 28, there was no simple correlation between the RFUs for each polymer and series with its contact angles. Both high and low RFUs were observed at contact angles around 67°- 77°.

3.4. Discussion

As hypothesized, and unlike the ACR-HEMA copolymers, a variation in surface wettability for the ACR-BMA/-MMA/-BMA-MMA polymers was observed. Although the relationship between increasing ACR content and contact angles was non-linear, the

repetition of the trend in all three polymer series suggests the changes were a consequence of the changing ACR content and to a lesser degree the hydrophobic constituent(s) of the polymers. A possible explanation for observing contact angles of 67°- 77° at high and low weight percentages of ACR and angles of 27.6°- 42.9° at 60 wt% ACR is outlined in Figure 29.

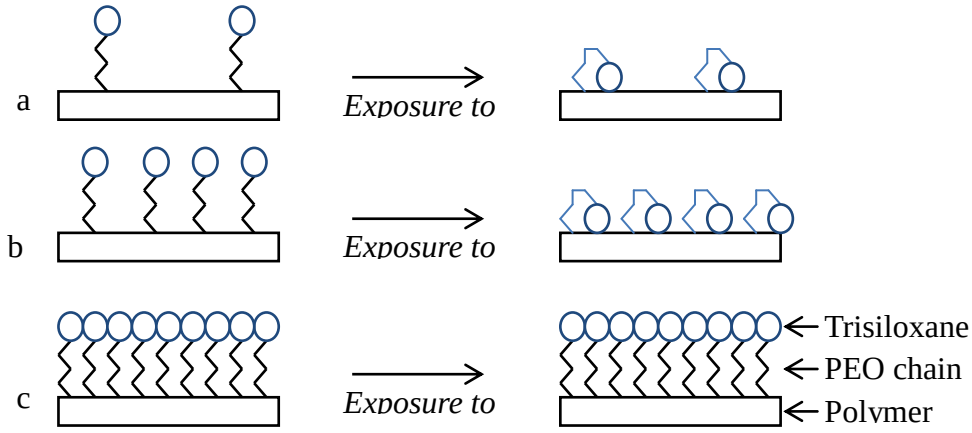

Figure 29: Proposed mechanistic explanation for low contact angles (27.6°- 42.9°) observed only at moderate weight percentages of ACR (20 < x < 80 wt% ACR) with a) representing low wt %, b) moderate wt %, and c) high wt% ACR content.

Trisiloxane based surfactants, such as ACR, have a propensity for migration to the air-polymer interface.[44] It is hypothesized that upon hydration, the flexible and exposed parts of the PEO chains[167] in the surfactant rotate to minimize contact between water and the hydrophobic head groups [Figure 29.a]. If this is the case, it follows then that between certain weight percentages of ACR in the polymer, there are enough soluble PEO chains[168] reorienting at the surface [Figure 29.b] to confer hydrophilicity to the material, and thereby facilitate the spreading of water that results in the decreased contact angles seen in Figure 25. At higher weight percentages of ACR (~ ≥ 80 wt%) steric hindrance

from the close packing of PEO chains and trisiloxane heads may be preventing rotation of the surfactant molecule [Figure 29.c], which would present a hydrophobic layer to water and translate to high contact angles 67°- 77° for the polymer surfaces. It is important to note that a material's surface wettability can be decreased without chemical modification of the surface; an increase in surface roughness would also yield high contact angles.[105] Although this parameter was not quantitatively measured for these polymers, qualitative observation suggested highly smooth surfaces for all polymers in each of the three series. Hence, the dependence of varying surface wettability on ACR content for this set may be safely assumed.

Similarly the weight percent of ACR is highly influential on the water uptake, which increases with increasing ACR content of the polymers [Figure 26]. As was the case with the ACR-HEMA copolymers, the 'bulky' PEO of the ACR segments may be creating greater space in the matrix for water absorption than the smaller BMA and MMA polymers, while facilitating inwards osmosis due to their hydrophilic nature. The minimal water uptake seen by poly-MMA and poly-BMA emphasizes the necessity of a hydrophilic constituent in materials that imbibe water,[169] even though hydrogels containing a significant amount of hydrophobic polymers are possible.[116] Hence, the positive correlation between weight percent of ACR and swelling in the ACR-MMA-BMA polymers is unsurprising.

The increasing *E. coli* adhesion observed with increasing weight percent ACR, however, was a surprise, given the previously described antibacterial activity of the ACR monomer [2.4.2.2]. The trend clearly does not correlate with surface wettability [Figure

28] and increasing ACR content in these terpolymers increases their pliability, which should decrease adhesion as suggested by the literature [2.4.1.2]. It seems then that the adhesion results may be connected with the percent water uptake, since it mimics the fluorescence trend for the ACR-MMA-BMA series [Figure 26]. Whether or not this is a statistically significant correlation needs to be determined since the water uptake data for the ACR-BMA and ACR-MMA series needs to be acquired. Equally, the reason for occasional adhesion differences between copolymers of the three series requires further examination.

3.5. Conclusions

The evidently changing contact angles for the ACR-BMA, ACR-MMA and ACR-MMA-BMA polymers and the proposed mechanistic explanation validate the prerequisite hypothesis of chapter 2; namely that the tendency of trisiloxanes to occur at the interface[44] and their systematic variance therein can produce controlled wettability of the surface, provided of course, that the polymerization reaction is optimized to ensure ACR participation. Although the wettability for these polymers did not correlate with adhesion of *E. coli*, increasing the system's ACR content did increase water uptake, a trend that was similar to that of adhesion against increasing weight percent ACR. Such an observation has implications for antifouling surfaces, which may be improved if made from materials that do not imbibe water.

4. CONCLUSION

Bacterial biofilms are problematic for a number of reasons in multiple industries, but particularly in the biomedical context where their formation on implanted biomaterials can result in device failure with significant economic implications.[13,14] As such the development of biofilm-mitigating surfaces has received significant attention, and there is a growing understanding that a combination of strategies may produce the most efficacious antibacterial material.

To this end, novel types of polymers were synthesized using an acrylate-modified silicone surfactant (ACR) and either a hydrophilic component (HEMA) or hydrophobic monomers (BMA, MMA or BMA and MMA) in the hope of studying bacterial adhesion as a function of surface wettability, since knowing the relationship between these two variables could direct the synthesis of eventual antifouling surfaces. The first set of ACR-HEMA copolymers was highly transparent within the range of visible light wavelengths, but had consistent hardness, roughness, wettability and consequently *E. coli* adhesion despite changes in the bulk composition of the materials. Hence, it was impossible to discern the effect of varying surface wettability on bacterial adhesion as initially hypothesized. The lack of variance in contact angles was likely due to 1) an imperfect polymerization process evidenced by the significant loss of ACR after propanol-based extraction, and 2) the homogenous dispersion in the system of the remaining ACR, both of which resulted in a consistent interface. This problem may be circumvented by using a better photoinitiating system to ensure adequate participation of ACR in the polymer matrix.

Although initial adhesion of bacteria is a prerequisite to biofilm formation, and *E. coli* clearly adhered to the copolymers, the anti-bacterial activity of ACR and HEMA monomers apparent in the Kirby-Bauer test was promising and necessitates the use of a live-dead stain to ascertain the percentage of adhered *E. coli* cells that are live versus dead on the copolymer surfaces. Calculating such percentages would require a quantification of adhered versus non-adhered cells, and so the immediate next steps involve the plotting of a standard growth curve, where the optical density of serial dilutions from a known concentration of *E. coli* solution are measured and correlated with colony counts from plating each dilution. The subsequent comparison of quantitative data with known antibacterial materials may also be of value when qualifying the overall efficacy of the ACR-HEMA copolymers as candidates for antifouling surfaces.

Unlike the first set, varying the weight percent of ACR in the ACR-MMA-BMA, ACR-MMA and ACR-BMA polymer series allowed controlled surface wettability that did not correlate with *E. coli* attachment to the same. It did, however, have a positive association with both water uptake and relative adhesion suggesting a correlation between the two. Validation of this hypothesis would require measurement of percent water uptake for each of the ACR-BMA and ACR-MMA copolymer sets, and the subsequent plotting of the data against their observed relative GFP fluorescence with accompanying statistical analysis. This work in conjunction with the potential link between bacterial adhesion and percent water uptake of ACR-BMA/-MMA/-BMA-MMA materials, as well as the potential antimicrobial activity of ACR-HEMA copolymers (pending the use of a live-

dead stain) , may provide a way to increase the efficacy of antifouling materials, not limited to the biomedical industry.

REFERENCES

[1] Olsen, M.E., Ceri, H., Morck, D.W., Buret, A.G. and Read, R.R. (2002). Biofilm bacteria: formation and comparative susceptibility to antibiotics, *Can J Vet Res*, **66:** 86-92.

[2] Freitas, R.A. and Merkle, R.C. (2004). *Kinematic Self-Replicating Machines*, Landes Bioscience, Georgetown, TX.

[3] Mah, F.C. and O'Toole, G.A. (2001). Mechanisms of biofilm resistance to antimicrobial agents, *Trends Microbiol*, **9**:34–39.

[4] Costerton, J.W. (1994). Biofilms- the customized micronice. *Am Soc Microbiol,* **176** (8): 2137-2142**.**

[5] Lewis, K. (2001). Riddle of biofilm resistance. *Antimicrob Agents Chemother*, **45:**999–1007.

[6] Magot, M. and Ollivier, B. (2005). *Petroleum microbiology,* ASM Press, Washington, D.C.

[7] Holah, J.T., Betts, R.P. and Thorpe, R.H. (1989). The use of epifluorescence microscopy to determine surface hygiene. *Int Biodeteriorat,* **25:** 147–153.

[8] Carpentier, B. (1993). Biofilms and their consequences, with particular reference to hygiene in the food industry. *J Appl Bacteriol*, **75:** 499–511.

[9] Mahenthiralingam, E., Campbell, M.E. and Speert, D.P. (1994). Nonmotility and phagocytic resistance of *Pseudomonas aeruginosa* isolates from chronically colonized patients with cystic fibrosis. *Infect Immun,* **62:** 596–605.

[10] Donlan, R.M. and Costerton, J.W. (2002). Biofilms: survival mechanisms of clinically relevant microorganisms, *Clin Microbiol Rev,* **15:**167–193.

[11] Stewart, P.S., Mukherjee, P.K. and Ghannoum, M.A. (2004). Biofilm antimicrobial resistance. In M. Ghannoum and G.A. O'Toole (eds), *Microbial Biofilms* (p. 250–268). Washington: ASM Press.

[12] Donlan, R.M. (2008). Biofilms on central venous catheters: is eradication possible? In Romeo, T. (ed), *Curr Top Microbiol Immun: Bacterial Biofilms.* (p. 133–161). Berlin: Springer-Verlag.

[13] Neu, T.R. (1992). Biodeterioration of medical-grade silicone rubber used for voice prostheses: a SEM study. *Biomaterials,* **14**(6): 459-464.

[14] Darouiche, R.O. (2004). Treatment of infections associated with surgical implants. *N Eng J Med,* **350**:1422–1429.

[15] Steele, A. (2008). Impact of jerry can disinfection in camp environment– experiences in an IDP camp in Northern Uganda. *J Water and Health,* **6**(4): 559-564.

[16] Jung, D.R., Kapur, R., Adams, T., Giuliano, K.A., Mrksich, M., Craighead, H.G. and Taylor, D.L. (2001). Topographical and physiochemical modification of material surface to enable patterning of living cells. *Crit Rev in Biotech,* **21**(2): 111-154.

[17] Ratner, B.D., Hoffman, A.S., Schoen, F.J. and Lemons, J.E. (2004). *Biomaterials Science: An Introduction to Materials in Medicine.* (2nd ed.) San Diego, CA: Elsevier Academic Press.

[18] Thibon, P. Le Coutour, X., Leroyer, R. and Fabry, J. (2000). Randomized multi-centre trial of the effects of a catheter coated with hydrogel and silver salts on the incidence of hospital-acquired urinary tract infections. *J Hosp Infect,* **45:**1117–1124.

[19] Hetrick, E.M. and Schoenfisch, M.H. (2006). Reducing implant-related infections: active release strategies. *Chem Soc Rev,* **35**(9): 780-789.

[20] Zilberman, M. and Elsner, J.J. (2008). Antibiotic-eluting medical devices for various applications. *J Control Release,* **130(**3): 202-215.

[21] LeVier, R.R., Harrison, M.C., Cook, R.R. and Lane, T.H. (1993). What is silicone? *Plast Reconstr Surg*, **92**:163-67.

[22] Brook, M.A. (2000). Silicones. In *Silicon in Organic, Organomettalic, and Polymer Chemistry.* New York, NY: John Wiley & Sons Inc.

[23] Interrante, L.V., Shen, Q. and Li, J. (2001). Poly(dimethylsilylenemethylene-co-dimethylsiloxane): A Regularly Alternating Copolymer of Poly(dimethylsiloxane) and Poly(dimethylsilylenemethylene). *Macromolecules,* **34**(6): 1545-1547.

[24] Park, J.H., Park, K.D. and Bae, Y.H. (1999). PDMS-based polyurethanes with MPEG grafts: synthesis, characterization and platelet adhesion study. *Biomaterials,* **20**: 943-953.

[25] Mata, A., Fleischman, A.J. and Roy, S. (2005). Characterization of polydimethylsiloxane (PDMS) properties for biomedical micro/nanosystems. *Biomed Microdevices,* **7**(4): 943-953.

[26] Ertel, S.I., Ratner, B.D., Kaul, A., Schway, M.B. and Horbett, T.A. (1994). In vitro study of the intrinsic toxicity of synthetic surfaces to cells. *J Biomed Mat Res,* **28**(6): 667-675.

[27] Van Kooten, T.G., Whitesides, J.H. and von Recum, A.F. (1998). Influence of silicone (PDMS) surface texture on human skin fibroblast proliferation as determined by cell cycle analysis. *J Biomed Mat Res,* **43**(1): 1-14.

[28] Kunnavakkam, M.V., Houlihan, F.M., Schlax, M., Liddle, J.A., Kolodner, P., Nalamasu, O. and Rogers, J.A. (2003). Low-cost, low-loss microlens arrays fabricated by soft-lithography replication process. *Appl Phys Let,* **82**(8): 1152-1154.

[29] Vallet-Regi, M. and Balas, F. (2008). Silica materials for medical applications. *The Open Biomedical Engineering Journal,* **2**: 1-9.

[30] Boelens, J.J., Tan, W-F., Dankert, J. and Zaat, S.A.J. (2000). Antibacterial activity of antibiotic-soaked polyvinylpyrrolidone-grafted silicone elastomer hydrocephalus shunt. *J Antimicrob Chemother,* **45**(2): 221-224.

[31] Levy, M.L., Luu, T., Meltzer, H.S., Bennett, R. and Bruce, D.A. (2004). Bacterial adhesion to surfactant-modified silicone surfaces. *Neurosurgery,* **54**(2): 488-90.

[32] Tang, H., Cao, T., Wang, A., Liang, X., Salley, S.O., McAllistor, J.P. and Ng., K.Y.S. (2007). Effect of surface modification of silicone on *Staphylococcus epidermidis* adhesion and colonization. *J Biomed Mat Res Pt A,* **80**(4):885-94.

[33] Menaa, B., Miyagawa, Y.m Takahashi, M., Herrero, M., Rives, V., Menaa, F. and Eggers, D.K. (2009). Bioencapsulation of apomyoglobin in nanoporous organosilica sol-gel glasses: influence of the siloxane network on the conformation and stability of the model protein. *Biopolymers,* **91**(11): 895-906.

[34] Kim, T., Slowing, I.I., Chung, P.W. and Lin, V.S. (2011). Ordered mesoporous polymer-silica hybrid nanopoarticles as vehicles for the intracellular controlled release of macromolecules. *ACS-Nano,* **5**(1): 360-366.

[35] Müller, W.E., Engel, S., Wang, X., Wolf, S.E., Tremel, W., Thakur, N.L., Krasko, A., Divekar, M. and Schröder, H.C. (2008). Bioencapsulation of living bacteria (*Escherichia coli*) with poly(silicate) after transformation with silicatein-alpha gene. *Biomaterials,* **29**(7):771-779.

[36] Dufréne, Y.F., Boonaeart, C.J-P. and Rouxhet, P.G. (1996). Adhesion of *Azospirillum brasilense*, role of proteins at the cell-support interface. *Colloides Surf, B*: **7**(3): 113–128.

[37] Hüsmark, U. and Rönner, U. (1992). The influence of hydrophobic, electrostatic, and morphologic properties on the adhesion of *Bacillus* spores. *Biofouling*, **5**: 335–344.

[38] Teixera, P. and Oliveira, R. (1999). Influence of surface characteristics on the adhesion of *Alcaligenes denitrificans* to polymeric substrates. *J Adhes Sci Technol,* **13**: 1287–1294.

[39] Sinde, E. and Carballo, J. (2000). Attachment of *Salmonella* spp., and *Listeria monocytogenes* to stainless steel, rubber and polytetrafluorethylene : the influence of free energy and the effect of commercial sanitizers. *Food Microbiol. (Lond.)* **17**: 439–447.

[40] Owen, M.J. and Dvornic, P.R. (2012). *Chapter 9* in *Silicone Surface Science Vol.4.* Retrieved from DOI: 10.1007/978-94-007-3876-8.

[41] Giraldez, M.J., Resua, C.G., Lira, M., Oliveria, M.E., Magarinos, B., Toranzo, A.E. and Yebra-Pimentel, E. (2010). Contact lens hydrophobicity and roughness effects on bacterial adhesion. *Optom Vis Sci*, **87**(6): E426-431.

[42] Kodjikian, L., Burillon, C., Roques, C., Pellon, G., Frenery, J. and Renaud, F.N.R. (2003). Bacterial adherence of *Staphylococcus epidermidis* to intraocular lenses: A bioluminescence and scanning electron microscopy study. *IOVS*, **44**(10): 4388-4394.

[43] Kolarík, J. and Migliaresi, C. (1983). Mechanical properties of hydrophilic copolymers of 2-hydroxyethyl methacrylate with ethyl acrylate, n-butyl acrylate, and dodecyl methacrylate. *J Biomed Mater Res*, **17**(5): 757-767.

[44] Wagner, R., Wu, Y., Czichocki, G., Berlepsch, H.V., Weiland, B., Rexin, F. and Perepelittchenko, L. (1999). Silicon-modified surfactants and wetting: I. Synthesis of the single components of Silwet L77 and their spreading performance on a low-energy solid surface. *Appl Organomet Chem*, **13**(9):611–620.

[45] Life Technologies (n.d.). Freezing Cells. Retrieved from http:// http://www.invitrogen.com/site/us/en/home/References/gibco-cell-culture-basics/cell-culture-protocols/freezing-cells.html

[46] Remington: science and practice of pharmacy- chapter 36- Separation-pg.695- Lippincott Williams & Wilkins, 2005- 21st edition.

[47] Bruinsma, G.M., van der Mei, H.C. and Busscher, H.J. (2001). Bacterial adhesion to surface hydrophilic and hydrophobic contact lenses. *Biomaterials*, **22:** 3217- 3224.

[48] Katsikogianni, M. & Missirlis, Y.F. (2004). Bacterial adhesion and proliferation on biomaterials. Techniques to evaluate adhesion process. The influence of surface chemistry/topography. *European cells and Materials, 7*: 38.

[49] Lensen, M.C., Schukte, V.A., Salber, J., Diez, M. Menges, F., Moller, M. (2008). Cellular responses to novel, micropatterned biomaterials. *Pure and Applied Chemistry*, **80**(11): 2479-2487.

[50] Yu, F.Y., Mucklich, F., Li, P., Shen, H. Mathur, S. Lehr, C.M. and Bakowsky, U. (2005). *In vitro* cell response to a polymer surface micropatterned by laser interference lithography. *Biomacromolecules*, **6**(3): 1160-1167.

[51] Mitik-Dineva, N., Wang, J., Truong, V.K., Stoddart, P., Malherbe, F., Crawford, R.J. and Ivanova, E.P. (2009). *Escherichia coli*, *Pseudomonas aeruginosa* and *Staphylococcus aureus* attachment patterns on glass surfaces with nancoscale roughness. *Curr Microbiol*, **58**: 268-273.

[52] Ivanova, E.P., Truong, V.K., Wang, J., Berndt, C.C., Jones, T.R., and Yusuf, I.I. (2010). Impact of nanoscale roughness of titanium thin films surfaces on bacterial retention. *Langmuir*, **26:** 1973-1982.

[53] Tang, H., Cao, T., Liang, X., Wang, A., Salley, S.O., McAllister, J. and Ng, S. (2008). Influence of silicone surface roughness and hydrophobicity on adhesion and colonization of *Staphylococcus epidermidis*. *J Biomed Mater Res Pt A*, **88A**(2): 454-463.

[54] Gallardo-Moreno, A.M., Gonzalez-Martin, M.L., Bruque, J.M. and Perez-Giraldo, C. (2004). The adhesion strength of *Candida parapsilosis* to glass and silicone as a function of hydrophobicity, roughness and cell morphology. *Colloids Surf A Physiochem Eng Aspects*, **249**: 99-103.

[55] Quirynen, M., Vandermei, H.C., Bollen, C.M.L., Schotte, A., Marechal, M., Doornbusch, G.I., Naert, I., Busscher, H.J. and Vansteenberghe, D.A. (1993). An *in vivo* study of the influence of the surface-roughness of implants on the microbiology of supraginvial and subgingival plaque. *J Dent Res*, **72**: 1304-1309.

[56] Mcallister, E.W., Carey, L.C., Brady, P.G., Heller, R. and Kovacs, S.G. (1993). The role of polymeric surface smoothness of biliary stents in bacterial adherence, biofilm deposition and stent occlusion. *Gastrointest Endosc*, **39**: 422-425.

[57] Meyle, J., Gütlig, K., Wolburg, H., von Recum, A.F. (1993). Fibroblast anchorage to microtextured surfaces. *J Biomed Mats Res*, **27**(12): 1553-1557.

[58] Brunette, D.M. (1986). Fibroblasts on micromachined substrata orient hierarchically to grooves of different dimensions. *Exp Cell Res*, **164**(1): 11-26.

[59] Dunn, G.A. (1991). How do cells respond to ultrafine surface contours? *BioEssays*, **13**(10): 541-543.

[60] Jiang, X.Y., Takayama, S. Qian, X.P., Ostuni, E., Wu, H.K., Bowden, N., LeDuc, P., Ingber, D.E., (2002). Controlling mammalian cell spreading and cytoskeletal arrangement with conveniently fabricated continuous wavy features on poly(dimethysiloxane). *Langmuir*, **18**(8): 3273-3280.

[61] Biggs, M.J.P., Richards, R.G., Gadegaard, N., Wilkinson, C.D.W. and Dalby, M.J. (2007). Regulation of implant surface cell adhesion: Characterization and quantification of S-phase primary osteoblast adhesions on biomimetic nanoscale substrates. *J Ortho Res*, **25**: 273-282.

[62] Lee, J.N., Jiang, X., Ryan, D. and Whitesides, G.M. (2004). Compatibility of mammalian cells on surfaces of poly(dimethylsiloxane). *Langmuir*, **20**(26): 11684-11691.

[63] Parr, R.G. and Pearson, R.G. (1983). Absolute Hardness: companion parameter to electronegativity. *J Am Chem Soc*, **105**: 7512-7516.

[64] Brookes, C.A., Green, P., Harrison, P.H. and Moxley, B. (1972). Some observations on scratch and indentation hardness measurements. *J Phys D: Appl Phys*, **5**(7): 1284-1293.

[65] Briscoe, B.J., Evans. P.D., Biswas, S.K. and Sinha, S.K. (1996). The hardness of poly(methylmethacrylate). *Tribology International,* **29**(2): 93-104.

[66] Huang, J., Peng, X., Xiong, C. and Fang, J. (2011). Influence of substrate stiffness on cell-substrate interfacial adhesion and spreading: A mechano-chemical coupling model. *J Colloid Interf Science,* **355**: 503-508.

[67] Zamir, E. and Geiger, B. (2001). Molecular complexity and dynamics of cell-matrix adhesions. *J Cell Sci*, **114**: 3583-3590.

[68] Reinhart-King, C.A., Dembo, M. and Hammer, D.A. (2005). The dynamics and mechanics of endothelial cell spreading. *Biophys J*¸**89**(1): 676-689.

[69] Chan, C.E. and Odde, D.J. (2008). Traction dynamics of filopodia on compliant substrates. *Science,* **322**(5908): 1687-1691.

[70] Plant, A.L., Bhadriraju, K., Spurlin, T.A. and Elliot, J.T. (2009). Cell response to matrix mechanics: focus on collagen. *BBA- Molec Cell Res*¸**1793**(5): 893-902.

[71] Baker, E.L. and Zaman, M.H. (2010) The biomechanical integrin. *J Biomech*, **43**(1): 38-44.

[72] Choquet, D., Felsenfeld, D.P. and Sheetz, M.P. (1997). Extracellular matrix rigidity causes strengthening of integrin-cytoskeleton linkages. *Cell*, **88**(1): 39-48.

[73] Buxboim, A., Rajagopal, K., Brown, A.E.X. and Discher, D.E. (2010). How deeply cells feel: methods for thin gels. (2010). *J Phys Condens Matter,* **22**(19): 1-19.

[74] Yeung, T., Georges, P.C., Flanagan, L.A., Marg, B., Oritz, M. Funaki, M., Zahir, N., Ming, W.Y., Weaver, V., and Janmey, P.A. (2005). Effects of substrate stiffness on cell morphology, cytoskeletal structure and adhesion. *Cell Motil Cytoskel,* **60**(1): 24-34.

[75] Solon, J., Levental, I., Sengupta, K., Georges, P.C. and Janmey, P.A. (2007). Fibroblast adaptation and stiffness matching to soft elastic substrates. *Biophys J,* **93**(12): 4453-4461.

[76] Marklein, R.A. and Burdick, J.A. (2010). Spatially controlled hydrogel mechanics to modulate stem cell interactions. *Soft Matter*, **6**: 136-143.

[77] Lo, C.M. Wang, H.B., Dembo, M. and Wang, Y.L. (2000). Cell movement is guided by the rigidity of the substrate. *Biophys J*, **79**(1): 144-152.

[78] Sen, S., Engler, A.J. and Discher, D.E. (2009). Matrix strains induced by cells: computing how far cells can feel. *Cell Mol Bioeng*, **2**(1): 39-48.

[79] Ghibaudo, M., Saez, A., Trichet, L., Xayaphoummine, A., Browaeysm J., Silberzan, P., Buguin, A. and Ladoux, B. (2008). Traction forces and rigisity sensing regulate cell functions. *Soft Matter,* **4**: 1836-1843.

[80] Lichter, J.A., Thompson, M.T., Delgadillo, M., Nishikawa, T., Rubner, M.F. and Van Vliet, K.J. (2008). Substrata mechanical stiffness can regulate adhesion of viable bacteria. *Biomacromolecules,* **9**(6): 1571-1578.

[81] Cowles, K.N. and Gitai, Z. (2010). Surface association and the MreB cytoskeleton regulate pilus production, localization and function in the *Pseudomonas aeruginosa. Mol Microbiol,* **76**(6): 1411-1426.

[82] Dahlströmm, M., Jonsson, H., Jonsson, P.R. and Elwing, H. (2004). Surface wettability as a determinant in the settlement of the barnacle *Balanus Improvisus* (DARWIN). *J Exper Marine Bio Eco,* **305**: 223-232.

[83] Schlachter, I. And Feldmann-Krane, G. (1998). Silicone Surfactants. *Surfactants Sci Ser,* **74**: 201-239.

[84] Förch, R., Schönherr, H. and Jenkins, A.A.T. (Eds.). (2009). *Surface design: Applications in bioscience and nanotechnology.* Weinheim, Germany: Wiley-VCH.

[85] Hatch, J. (2006). Switchable surfaces; superhydrophillic to superhydrophobic. Abstract retrieved from: http://www.chemistry.illinois.edu/research/materials/seminar_abstracts/2006-2007/Hatch.abstract_copy.pdf

[86] Bair, R.E. (1984). Initial events in microbial film formation. In Costlow, J.D., Tipper, R.C. (eds.), *Marine Biodeterioration: An Interdisciplinary Study*. US Nav Inst, Annapolis, MD, pp. 57-62.

[87] Fletcher, M. and Pringle, J.H. (1985). The effect of surface free energy and medium surface tension on bacterial attachment to solid surfaces. *J Colloid Inter Sci,***104**: 5-14.

[88] Meyer, A.E., Baier, R.E. and King, R.W. (1988). Initial fouling of nontoxic coatings in fresh, brackish and seawater. *Can J Chem Eng,* **66**: 55–62.

[89] Arima, Y. and Iwata, H. (2007). Effect of wettability and surface functional groups on protein adsorption and cell adhesion using well-defined mixed self-assembled monolayers. *Biomat,* **28**(20): 3074-3082.

[90] Riberiro, M., Monteiro, F.J. and Ferraz, M.P. (2012). *Staphylococcus aureus* and S*taphylococcus epidermidis* adhesion to nanohydroxyapatite in the presence of model proteins. *Biomed Mater,* **7**(4): 045010.

[91] Tegoulia, V.A. and Cooper, S.L. (2002). *Staphylococcus aureus* adhesion to self-assembled monolayers: effect of surface chemistry and fibrinogen presence. *Col Surf B: Biointerf,* **24**: 217-228.

[92] Gui, B., Potter, K.A. and Capadona, J.R. (2012). In Y. Bar-Cohen (Eds.). *Biomimetics: Nature-based innovation.* (p. 95-129). Boca Raton, FL: CRC Press.

[93] Webster, T.J., Siegel, R.W., Bizios, R., Ergun, C. And Doremus, R.H. (2000). Specific proteins mediate enhanced osteoblast adhesion on nanophase ceramics. *J Biomed Mater Res A*, **51**: 475-483.

[94] Webster, T.J., Siegel, R.W., Bizios, R., Ergun, C. And Doremus, R.H. (2000). Enhanced functions of osteoblasts on nanophase ceramics. *Biomaterials*, **21**: 1803-1810.

[95] Christenson, E.M., Anseth, K.S. van den Beuken, J.J.J.P., Chan, C.K., Ercan, B., Jansen, J.A., Laurencin, C.T., LI, W-J., Murugan, R., Nair, L.S., Ramakrishna, S., Tuan, R.S. Webster, T.J. and Mikos, A.G. (2007). Nanobiomaterial applications in orthopedics. *J Orthop Res*, **25**: 11-22.

[96] Khang, D., Lu, J., Yao, C.H., Haberstroh, K.M. and Webster, T.J. (2008). The role of nanometer and sub-micron surface features on vascular and bone cell adhesion on titanium. *Biomaterials*, **29**: 970- 983.

[97] Liu, H., Yazici, H., Ergun, C., Webster, T.J. and Bermek, H. (2008). An *in vitro* evaluation of the Ca/P ratio for the cytocompatibility of nan-to-micron particulate calcium phosphate for bone regeneration. *Acta Biomateriala*, **4**: 1472-1479.

[98] Vandrovcova, M. and Bacakova, L. (2011). Adhesion, Growth and Differentiation of Osteoblasts on Surface-Modified Materials Developed for Bone Implants. *Physiol Res*, **60**: 403-417.

[99] Lensen, M.C., Schulte, V.A., Salber, J., Diez, M., Menges, F. and Moller, M. (2008). Cellular responses to novel, micropatterned biomaterials. *Pure Appl Chem*, **80**(11): 2479-2487.

[100] Richert, L., Vetrone, F., Yi, J-H., Zalzal, S.F., Wuest, J.D., and Rosei F. (2008). Surface nanopatterning to control cell growth. *Advan Mater*, **20**: 1488-1492.

[101] Mirzadeh, H., Shokrolahi, F. and Daliri, M. (2003). Effect of silicon rubber crosslink density on fibroblast cell behavior *in vitro*. *J Biomed Mater Res Part A*, **67 A**(3): 727-732.

[102] Truong, V.K., Lapovok, R., Estrin, Y.S., Rundell, S., Wang, J.Y., Fluke, C.J., Crawford, R.J. and Ivanova, E.P. (2010). The influence of nano-scale roughness on bacterial adhesion to ultrafine- grained titanium. *Biomaterials*, **31**: 3674-3683.

[103] Hay, K.M., Dragila, M.I., Liburdy, J. (2008). Theoretical model for the wetting of a rough surface. *J Colloid Interface Sci*, **325**: 472-477.

[104] Shibuichi, S., Onda, T., Satoh, N., Tsujii, K. (1996). Super water-repellent surfaces resulting from fractal surfaces.*J Phys Chem*, **100**:19512–19517.

[105] Veeramasuneni, S., Drelich, J., Miller, J.D., Yamauchi, G. (1997). Hydrophobicity of Ion-Plated PTFE Coatings. *Prog Org Coat*, **31**: 265-270.

[106] Extrand, C.W. (2004). Criteria for ultralyophobic surfaces. *Langmuir*, **20**: 5013-5018.

[107] Dendukuri, D., Panda, P., Haghgooie, R., Kim, J.M., Hatton, T.A. and Doyle, P.S. (2008). Modeling of Oxygen-Inhibited Free Radical Photopolymerization in a PDMS Microfluidic Device. *Macromolecules*, **41**: 8547-8556.

[108] O'Brien, A.K. and Bowman, C.N. (2006). Modeling the effect of oxygen on photopolymerization kinetics. *Macromol Theory Simul,* **15**: 176- 182.

[109] Pavia, D.L., Lampman, G.M., Kriz, G.S. and Vyvyan, J.R. (2009). *Introduction to Spectroscopy*. (p. 412). Belmont, CA: Books/Cole, Cengage Learning.

[110] Campo, E.A. (2008). *PDL Handbook series- Selection of Polymeric Materials: How to select design properties from different standards.* Norwich, NY: William Andrew Inc.

[111] Pierce, A. (1989). *Acoustics: an introduction to its physical principles and applications.* Melville, NY: Acoustical Society of America.

[112] Division of Ophthalmic Devices, Food and Drug Administration (n.d.). *Guidance for Industry and FDA Reviewers; Intraocular Lens Guidance Document*. Retrieved from http://www.fda.gov/OHRMS/DOCKETS/98fr/994052gd.pdf

[113] Young, J.M. (1988). AR coating: a definition. *Optical world,* **17**: 8-12.

[114] Park, J.H. and Bae, Y.H. (2002). Hydrogels based on poly(ethylene oxide) and poly(tetramethylene oxide) or poly(dimethyl siloxane): synthesis, characterization, *in vitro* protein adsorption and platelet adhesion. *Biomaterials,* **23**: 1797-1808.

[115] Gemeinhart, R.A. and Guo, C. (2004). Fast Swelling Hydrogel Systems. In N. Yui, R.J. Mrsny and K. Park (Eds.). *Reflexive polymers and hydrogels: understanding and designing fast responsive polymeric systems.* (p. 245-257). Boca Raton, FL: CRC Press.

[116] Ganji, F., Vasheghani-Farahani, S. and Vasheghani-Farahani, E. (2010). Theoretical description of hydrogel swelling: a review. *Iranian Polymer Journal,* **19**(5): 375-398.

[117] Kandavilli, S., Nair, V. and Panchagnula, R. (2002). Polymers in transdermal drug delivery systems. *Pharmaceutical Tech,* pp. 62-80. Retrieved from http://www.pharmtech.com/pharmtech/data/articlestandard/pharmtech/192002/18600/article.pdf

[118] Greenwood, J. and Johnson, K. (1981). *The Mechanics of Adhesion.* Amsterdam: Elsevier.

[119] Creton, C. And Papon, E. (2003). Materials Science of adhesives: how to bond things together. *Mater Sci,* **26**(8): 419-423.

[120] Carelli, C., Déplace, F., Boissonnet, L., Creton, C.J. (2007). Effect of a gradient in Viscoelastic properties on the debonding mechanisms of soft adhesives. *J Adhes,* **83**: 491-505.

[121] Creton, C., Hooker, J. and Shull, K.R. (2001). Mechanisms of soft adhesives: extension to large strains. *Langmuir*, **17**: 4948-4954.

[122] Shull, K.R. and Creton, C.J. (2004). Deformation behavior of thin compliant layers under tensile loading conditions. *Polym Sci Pt B: Polym Phys*, **42**: 4023–4043.

[123] Chiche, A.; Creton, C. (2004). *Proceeding of the 27th Annual Adhesion Society Meeting; Wilmington, NC.* pp. 296-298.

[124] Herman, K. (2011). *Hardness Testing: Principles and Applications.* Materials Park, OH: ASM International.

[125] Brown, R.P. (1996). *Physical testing of rubber- 3rd Edition.* Boundary Row, London: Chapman & Hall.

[126] Mittal, K.L. (Eds.). (2009). *Contact angle, wettability and adhesion.* (Vol. 6). Leiden, The Netherlands: Koninklijke Brill NV.

[127] Block, S.S. (2001). *Disinfection, Sterilization and Preservation.* Philadelphia, PA: Lippincott Williams & Wilkins.

[128] Bauer, A.W., Perry, D.M. and Kirby, W.M.M. (1959). Single disc antibiotic sensitivity testing of Staphylococci. *Arch Int Med,* **104**:208-216.

[129] Bauer, A.W., Kirby, W.M., Sherris, J.C. andTurck, M. (1966). Antibiotic susceptibility testing by a standardized single disk method.*Amer J Clin Pathol,* **45**(4):493-496.

[130] Petersdorf, R.G. and Sherris, J.C. (1965). Methods and significance of in vitro testing of bacterial sensitivity to drugs. *Amer J Med,* **39**:766-779.

[131] Varesano, A., Vineis, C. Aluigi, A. and Rombaldoni, F. (2011). Antimicrobial polymers for textile products. In A. Méndez-Vilas (Ed.), *Science against microbial pathogens: communicating current research and technological advances.* Biella, Itlay: CNR-ISMAC.

[132] Hudzicki, J. (2012). Kirby-Bauer disk diffusion susceptibility test protocol. Retrieved from http:// http://www.microbelibrary.org/component/resource/laboratory-test/3189-kirby-bauer-disk-diffusion-susceptibility-test-protocol

[133] Sezonov, G., Joseleau-Petit, D. and D'Ari, R. (2007). *Escherichia coli* physiology in Luria- Bertani Broth. *J of Bateriology,* **189**(23): 8746- 8749.

[134] Edwards, K. and Almgren, M. (1992).Surfactant-induced leakage and structural-change of lecithin vesicles-effect of surfactant headgroup size. *Langmuir*, **8**(3): 824-832.

[135] López, O., Cóceram M., Coderch, L., Parra, J.L., Barsukoc, L. and de la Maza, A. (2001). Octyl glucoside-mediated solubilization and reconstitution of liposomes: Structural and kinetic aspects. *J Phys Chem B,* **105**(40): 9879-9886.

[136] Polozova, A.I., Dubachev, G.E., Simonova, T.N. and Barsukov, L.I. (1995). Temperature-induced micellar lamellar transformation in binary-mixtures of saturated phosphatidylcholines with sodium cholate. *Febs Lett,* **358**(1): 17-22.

[137] Silvander, M., Karlsson, G. and Edwards, K. (1996). Vesicle solubilization by alkyl sulfate surfactants: a cryo-TEM study of the vesicle to micelle transition. *J Colloid Interface Sci,* **179**(1): 104-113.

[138] Pata, V., Ahmed, F., Discher, D.E. and Dan, N. (2004). Membrane solubilization by detergent: resistance conferred by thickness. *Langmuir,* **20**: 3888-3893.

[139] Kragh-Hansen, U., le Maire, M. and Moller, J.V. (1998). The mechanism of detergent solubilization of liposomes and protein-containing membranes. *Biophys J,* **75**(6): 2932-2946.

[140] Lichtenberg, D., Robson, R.J. and Dennis, E.A.(1983). Solubilization of phospholipids by detergents structural and kinetic aspects. *Biochmi Biophys Acta (BBA)- Rev Biomembr,* **737**(2): 285-304.

[141] Ba, Y. and Lasic, D.D. (Eds). (1995). *Liposomes as a model for solubilization and reconstitution of membranes.* Boca Raton, FL: CRC Press.

[142] Jackson, M.L., Schmidt, C.F., Lichtenberg, D., Litman, B.J. and Albert, A.D. (1982). Solubilization of phophatidylcholine bilayers octylglucoside. *Biochemistry,* **21:** 4576-4582.

[143] Moller, J.V. and Maire, M.L. (1993). Detergent binding as a measure of hydrophobic surface area of integral membrane proteins. *J Biol Chem,* **268**(25): 18659-18672.

[144] Paternostre, M., Meyer, O., Gabriele-Madelmont, C., Lesieur, S., Ghanam, M. and Ollivon, M. (1995). Partition coefficient of a surfactant between aggregates and solution: application to the micelle-vesicle transition of egg phosphatidylcholine and octyl beta-D-glucopyranoside. *Biophys J,* **69**(6): 2476-2488.

[145] Lévy, D., Bluzat, A., Seigneuret, M. and Rigaud, J-L. (1990). A systematic study of liposome and proteoliposome reconstitution involving Bio-Bead-mediated Triton X-100 removal. *Bioch Biophys Acta,* **1025**: 179-190.

[146] Nomura, F., Nagata, M., Inaba, T., Hiramatsu, H., Hotani, H. and Takiguchi, K. (2001). Capabilities of liposomes for topological transformation. *PNAS,* **98**(5): 2340-2345.

[147] Yoshii, E. (1996). Cytotoxic effects of acrylates and methacrylates: relationships of monomer structures and cytotoxicity. *J Biomed Mater Res,* **37**(4): 517-524.

[148] Paranjpe, A., Bordador, L.C.F., Wang, M-Y., Hume, W.R. and Jewett, A. (2005). Resin Monomer 2-Hydroxyethyl Methacrylate (HEMA) is a potent inducer of apoptotic cell death in human and mouse cells. *J Dent Res,* **84**(2): 172-177.

[149] Geyrsten, W., Lehman, F., Spahl, W. and Leyhausen, G. (1998). Cytotoxicity of 35 dental resin composite monomers/ additives in permanent 3T3 and three human primary fibroblast cultures. *J Biomed Mater Res,* **41**: 474-480.

[150] Ratanasathien, S., Wataha, J.C., Hanks, C.T. and Dennison, J.B. (1995). Cytotoxic interactive effects of dentin bonding components on mouse fibroblasts. *J Dent Res,* **74**: 1602-1607.

[151] Fujiswa, F., Kadoma, Y. and Komoda, Y. (1988). ^{1}H and ^{13}C NMR studies of the interaction of eugenol, phenol, and triethyleneglycol dimethacrylate with phospholipid liposomes as a model system for odontblast membranes. *J Dent Res,* **67**: 1438-1441.

[152] Fujisawa, S., Atsumi, T. and Kadoma, Y. (2001). Cytotoxicity and phospholipid-liposome phase-transition properties of 2-hydroxyehtyl methacrylate (HEMA). *Art Cells Blood Subs Immob Biotech,* **29**(3): 245-261.

[153] Li, B. and Logan, B.E. (2004). Bacterial adhesion to glass and metal-oxide surfaces. *Colloids Surf B: Biointerfaces* **36**: 81-94.

[154] Otto, K and Silhavy, T.J. (2002). Surface sensing of adhesion of *Escherichia* coli controlled by the Cpx-signalling pathway. *PNAS*, **99**(4): 2287-2292.

[155] Hulspas, R., O'Gorman, M.R.G., Wood, B.L., Gratama, J.W. and Sutherland, D.R. (2009). Considerations for the control of background fluorescence in clinical flow cytometry. *Cytometry Pt B,* **76B**: 355-364.

[156] Albano, C.R., Randers-Eichorn, L., Chang, Q., Bentley, W.E. and Rao, G. (1996). Quantitative measurement of green fluorescent protein expression. *Biotech Techniques,* **10**(12): 953-958.

[157] Thermo Scientific: Pierce Protein Biology Products. (2012). *Fluorescent probes*. Retrieved from http://www.piercenet.com/browse.cfm?fldID=4DD9D52E-5056-8A76-4E6E-E217FAD0D86B

[158] Lakowicz J.R. (Ed.) (2006). *Principles of Fluorescence Spectroscopy, Vol 1- 3rd Edition.*

[159] Kim, H-S., Song, X.J., de Paiva, C.S., Chen, Z., Pflugfelder, S.C. and Li, D-Q. (2004). Phenotypic characterization of human corneal epithelial cells expanded ex vivo from limbal explants and single cell cultures. *Biomaterials,* **79**: 41-49.

[160] Sundstrom, S., Scolnick, B. and Sullivan, J.B. (2001). Acrylates, Methacrylates and Cyanoacrylates. In J.B. Sullivan and G.R. Krieger (Eds.) , *Clinical Environmental Health and Toxic Exposures,* (pages 999-1005). Philadelphia, USA: Lippincott Williams & Wilkins.

[161] International Programme on Chemical Safety- World Health Organization (1998). Concise International Chemical Assessment Document No. 4- Methyl Methacrylate.

Retrieved from
http://www.inchem.org/documents/cicads/cicads/cicad04.htm#PartNumber:1

[162] Geslest, Inc. (2012). UV-Electron beam siloxane hybrid materials. Retrieved from: http://www.gelest.com/gelest/forms/GeneralPages/Applications/uv_eb.aspx

[163] Muratore, L.M. and Davis, T.P. (2000). Self-reinforcing hydrogels comprised of methyl methacrylate macromers copolymerized with *N,N*- Dimethylacrylamide. *J Polymer Sci: Pt A: Polymer Chem*, **38**: 810–817.

[164] Peng, D., Lu, G., Zhang, S., Zhang, X. and Huang, X. (2006). Novel amphiphilic graft copolymers bearing hydrophilic poly(acrylic acid) backbones and hydrophobic poly(butyl methacrylate) side chains. *J Polymer Sci Pt A: Polymer Chem*, **44**(23): 6857-6868.

[165] Fisher, J.P., Dean, D., Engel, P.S. and Mikos, A.G. (2001). Photoinitated polymerization of biomaterials. *Annu Rev Mater Res*, **31**(1): 171-181.

[166] Ahn, K.D., Chung, C.M. and Kim, Y.H. (1999). Synthesis and photopolymerization of multifunctional methacrylates derived from bis-GMA for dental application. *J Appl Polym Sci*, **71**:2033–2037.

[167] Yao, D., Kuila, T., Sun, K-B., Kim, N-H. And Lee, J-H. (2011). Effect of reactive poly(ethylene glycol) flexible chains on curing kinetics and impact properties of bisphenol-A glycidyl ether epoxy. *J App Polymer Sci*, **124**(3): 2325-2332.

[168] Harris, J.M. (Ed.). (1992). Poly (ethylene glycol) chemistry: biotechnical and biomedical applications. New York, NY: Plenum Press.

[169] Pal, K., Banthia, A.K. and Majumdar, D.K. (2009). Polymeric hydrogels: characterization and biomedical applications- a mini review. *Designed Monomers and Polymers*, **12**: 197-220.